

Pixel 2 People



NATIONAL REMOTE SENSING CENTRE
Indian Space Research Organisation

NEWSLETTER
January 2021

inform inspire educate engage innovate

Volume 10 Issue 1

from the directors's desk

Greetings. I am optimistic that all my NRSC colleagues and their families are safe from COVID-19. Though the administration of vaccine has commenced, the threat of Corona virus still persists and everyone needs to be vigilant and continue to follow precautions. Despite operations at different levels of staff attendance, NRSC has managed the functioning of the core operations of data acquisition; data processing & dissemination; support to ministries in different application projects along with training & outreach.



During the last six months, the establishment of 7.3m S/X/Ka remote sensing data reception antenna system (DRS2) at Bharati, Antarctica is made operational to support payload data reception and TTC for all IRS missions. We have successfully demonstrated the automation from first day payload acquisition in operational chain for the EOS-1 satellite sensor. The installation of NovaSAR hardware and integration of s/w with IMGEOs chain is completed and ANTRIX has declared the start of service for the data dissemination. Cartosat-3 data is declared operational for user community. The Fairbanks ground station was added to the pool of ISRO distributed ground network for processing of SCATSAT-1 data at IMGEOs and is operational.

NRSC has acquired around 11,066 satellite passes (efficiency above 99.9%) from which 2,85,744 data products were generated during last six months.

The Bhuvan content has been upgraded with 1m high resolution data (2018) covering 80% of India. The average hits of Bhuvan geoportal have increased from 1.1 crore to 2 crore hits/day and recorded 93,794 NOEDA downloads during this period. The Housing for all - Phase 2 application is made live. The PMGSY and Geographical Indications (GI) applications were made live during this period. The CDMA-Phase 2 application for Dept. of CDMA, Govt. of Telangana for property tax mapping of assessments, portions, trade, advertisements and cell towers for 134 ULB's is made live in January, 2021 and is awarded **Janaagraha City Governance Award**.

NRSC disseminated 151 flood products and 75 value added flood products for 9 states. Weekly and fortnightly locust bulletins are published and disseminated to the stake holders under operational Locust monitoring and early warning.

In the GOI flagship programme of AMRUT, pre-field mapping is completed for all the 239 cities and the final GIS database of 42 AMRUT cities is handed over to urban local bodies for formulation of GIS based master plans. The regional centres contributed for the identification of sites for sewage treatment plants in 5 small & medium size towns using geospatial techniques across the country. The crop surveillance information products and crop sowing intelligence information products were generated on fortnightly basis for kharif 2020 for the state of Maharashtra. Two new biogeochemical products, viz., dissolved inorganic carbon and total alkalinity, are released under NICES portal. High resolution DEM (10 mm accuracy) is generated to characterize lunar simulated craters using LiDAR mobile mapping system at Ullarthi, Chitradurga site.

A "Glacial Lake Atlas of Indus River Basin" was released by Secretary, DoWR, RD & GR through webinar. The sand dune atlas with comprehensive details of the sand dunes in Thar desert was also released.

The storage infrastructure, IMGEOs Storage Augmentation (SAN) & SAN bandwidth have been augmented for better dissemination of products. The ISO 9001:2015 recertification has been completed even in the COVID scenario. Implementation of NIC e-office e-file solution is in place across all campuses of NRSC.

NRSC is gearing up for the new remote sensing data policy, which is on the offing.

Dr. Raj Kumar, Director, NRSC

index

Sl. No.	Description	Page No.
1	Mobile mapping system for high resolution 3D geospatial applications	02
2	Spatial analysis of geotagged data for rural development and planning	03
3	Development of satellite based regional evaporative flux monitoring system for india	04
4	Ozone variability: influence by its precursors and meteorological parameters- an investigation	05
5	Changes in regional meteorology due to land use/land cover alterations	06
6	Bhuvan	07
7	Vicarious calibration activities augmentation for ISRO EO optical on orbit sensors using RadCalNet data	08
8	Applications validation of ICESat-2 photon data	10
9	Estimation of brine concentration in salt pans using geospatial technology	11
10	Real-time operational spatial flood early warning system for Tapi and Godavari rivers	12
11	Locust surveillance using geospatial technology	13
12	Monitoring of net primary productivity of cotton agroeco system in central india using remote sensing-based models	14
13	SUFALAM: Development of methodology for mapping of maize and bajra crops grown in kharif season	15
14	Classification of mangroves and mapping their health spatially using HYSIS data	17
15	Generation of geospatial database for notified forest lands of Karnataka state	19
16	Site suitability for groundwater recharge in hard-rock basaltic terrain	20



Mr. Vinod M Bothale, receiving National Geomatics Award for excellence - 2019



1. Mobile mapping system for high resolution 3D geospatial applications

AS&DMA, NRSC has inducted Mobile Mapping System (MMS) in August, 2020 to augment its existing surveying and mapping infrastructure to cater to urban mapping, 3D city modeling, highway infrastructure mapping and monitoring, forest biomass estimation, utility asset mapping etc.

MMS consists of LiDAR sensor for range measurement, GNSS/ Inertial Measuring Unit (IMU)/ Distance Measuring Indicator (DMI) for position and orientation and 360° digital camera for spherical imaging. The mobile laser scanner is a survey grade scanner with class 1 laser and is eye safe. The scanner has pulse repetition rate of 1 MHz with a scan rate of 250 lines/second, laser range of 420m at 80% reflectivity. The GNSS/IMU provides accurate system trajectory and continuous kinematic positioning for direct geo-referencing of the point cloud. The DMI records the speed of the vehicle, which improves the quality of the trajectory, especially during obstructions by overhead bridges, tunnels, etc.

MMS contains 360° spherical imaging system for imaging at an overall 30 MP resolution covering 90% of a full sphere along with the laser cloud data collection. The MMS is portable, self-calibrating and most commonly mounted on a vehicle (Figure 1.1), however it can be mounted on different platforms like four wheeler /boat/ATV/train also. Two rechargeable batteries of 80 AH rating provide power supply to the system for 8 hours of operation.



Figure 1.1: MMS mounted on NRSC vehicle

The LiDAR scanner measures the range information with 360° full circle field of view across track and the movement of the vehicle results in data collection in the along track direction.

The GNSS/IMU data collected by the MMS is differentially processed with respect to GNSS base station data collected during survey for estimating precise trajectory of the vehicle in terms of position and orientation. By combining the scanner range

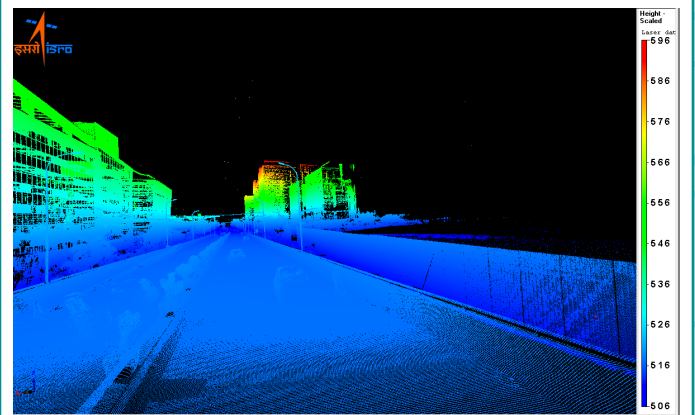


Figure 1.2: Georeferenced point cloud – near IKEA, Hyderabad measurements and post processed GNSS/IMU trajectory data, accurate 3D georeferenced point cloud is generated (Figure 1.2).

Additionally, LiDAR provides intensity information of the objects based on their reflectivity. Since the MMS has a 360° camera, the 360° panoramic images (Figure 1.3) are used to provide color information to the point cloud, by assigning RGB values to each and every point of the point cloud resulting in coloured 3D Point cloud (Figure 1.4).



Figure 1.3: 360° Panoramic image (Spherical view) – near IKEA, Hyderabad

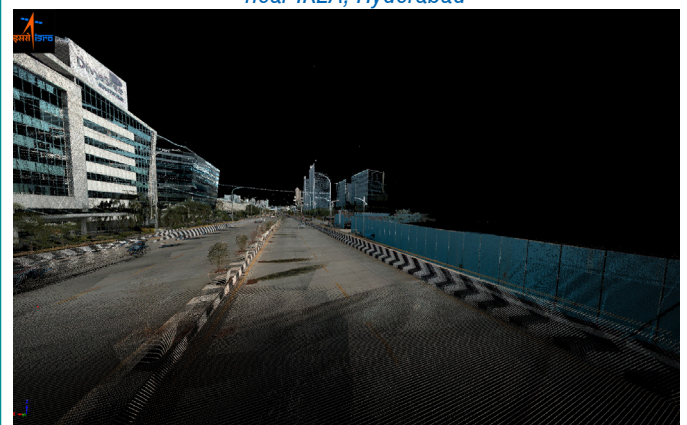


Figure 1.4: Colorized point cloud – near IKEA, Hyderabad

The scanner provides a very dense highly accurate point cloud and at vehicle speed of 80 kmph, it results in point spacing of 6 mm and 9cm in across and along track directions respectively.

The MMS applications are given in Table 1.1

Table 1.1: MMS applications

Type of Environment	Applications
Urban & Utilities	Urban mapping, 3D city models, street furniture mapping etc.
Road Network	Transport infrastructure mapping, corridor mapping, asset mapping, road inventory, structures and bridge clearance, etc.
Railway Network	Clearance mapping, track mapping, gradient analysis, tunnel mapping, landslide mapping, slope analysis, etc.
Forestry	Biomass estimation, canopy height models etc.
Opencast mining	Over burden mapping, change analysis, volumetric analysis etc.

2. Spatial analysis of geotagged data for rural development and planning

Spatial analysis has emerged as a basis of decision making and planning across various domains and sectors in recent years. Increased use of spatial analysis is also being witnessed in public service delivery and governance. A synergy between such tools and the human capabilities to analyze, envision, reason, and deliberate can be applied to derive crucial insights to the various rural development program implemented by the government, viz. MGNREGA, IWMP, RKVY, PDMC, etc.

MGNREGA project represents one of the largest repositories of over 4.3 crore geotagged rural assets. State level analysis of MGNREGA assets has been carried out with respect to existing Land Use Land Cover (LULC), slope and elevation along with spatial clustering of geotagged assets taking Uttarakhand as an example. During Phase 1 (2006-2017) 4,44,369 MGNREGA assets under different permissible work categories were created in the state and geotagged for visualization in Geo-MGNREGA Bhuvan portal. Land development in agriculture areas and flood control protection in forest areas have been found to be the most preferable works under MGNREGA in the state. In the habitation areas, rural sanitation works were found to be the most preferred ones. Thus, the distribution of assets has been found to be in accordance to the local requirements of rural communities, and it was also found to be incoherence with the state vision plan of 2030. Spatial clustering of the MGNREGA works using hot spot analysis has been carried out with the main focus of identifying clusters of villages with similar spatial density and a varying pattern has been observed in the 13 districts (Figure 2.1). The monitoring of the long term impacts of the project in the hot spots may yield more testimony to wide ranging benefits of MGNREGA, not only in enhancing the livelihood of the rural people but also in enhancing the resilience and overall development of the state. Further corroboration of works vis-à-vis UN 2030 Sustainable Development Goals (SDGs) beyond MGNREGA's most directly linked SDG i.e. SDG1-End Poverty has been also demonstrated

in spatially explicit manner (Figure 2.2). A composite SDG map harmonized with SDG India Index 2.0 classification was generated to highlight the sub-national district level spatial variations of indirect SDGs.

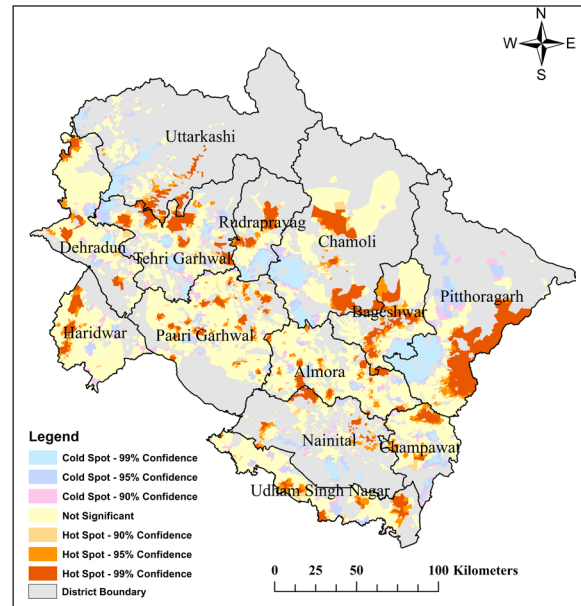


Figure 2.1: Spatial clustering of MGNREGA assets in Uttarakhand

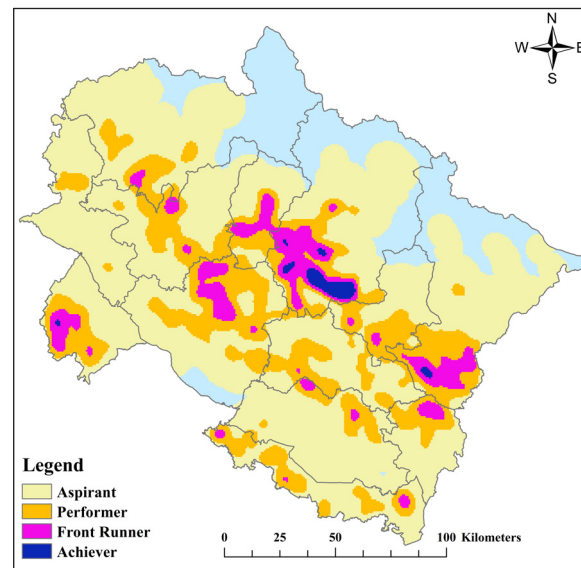


Figure 2.2: Composite SDG coverage under MGNREGA based on kernel density

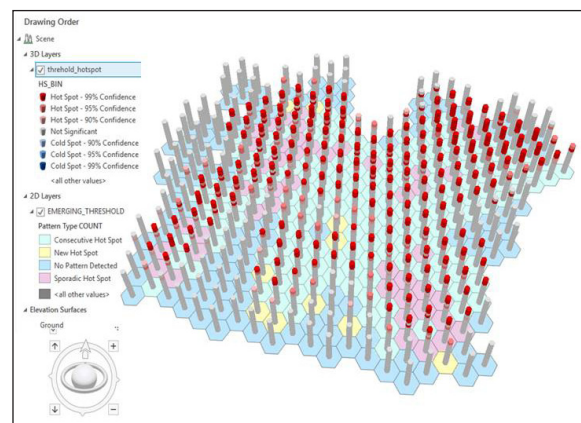


Figure 2.3: 3D Visualization of assets based on hotspot bins (Confidence levels) in Prakasam district, A.P.



In GIS, 3D visualization offers improved insight into complex data-sets as information can be displayed and interpreted more effectively. To demonstrate this, a rapid reconstruction of 3D visualization was performed on the MGNREGA assets in Prakasam district, Andhra Pradesh taking work completion year as the third dimension (Figure 2.3).

Two variants were generated based on the asset values and the Hotspot bins. The study showcased the potential utility of data driven and geo-intelligent analytics for temporal distribution of enormous number of the assets in an interactive way, which is otherwise not achievable in conventional 2D representation (Figure 2.4).

The ministry of Rural Development has been keen on using GIS based inputs along with the geotagged data for preparing the annual action plans for the gram panchayats for proposing the future activities. To achieve this, a geospatial planning portal Yuktdhara has been developed as a part of Bhuvan. The portal facilitates gram panchayat level planning of MGNREGA activities by integrating a wide variety of spatial information contents using open source GIS tools. Current level of integration incorporates multi temporal high resolution IRS satellite data in natural color, digital terrain, thematic layers as well as complete geotagged MGNREGA and Integrated

Watershed Management Project (IWMP) works across the country in a pro-convergence manner. Wide-ranging national level legacy datasets prepared by NRSC, such as LULC, roads and streams, ground water prospecting, geomorphology, wastelands, land degradation etc. strengthen the planning approach.

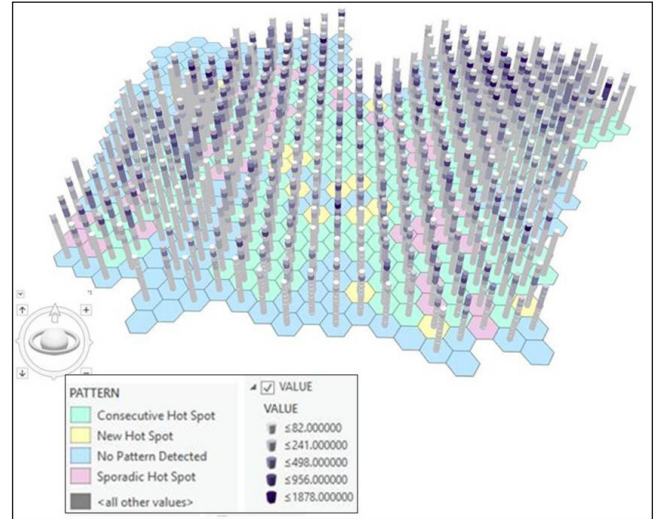


Figure 2.4: 3D Visualization of assets based on value bins (Joint count / Asset count) in Prakasam district, A.P.

3. Development of satellite based regional evaporative flux monitoring system for India

Water resources and agricultural management applications require evapotranspiration (ET) information over a range of spatial and temporal scales. ET can be defined as a collective term for all the processes by which water at or near the land surface becomes atmospheric water vapour. ET losses are one of the main components of the environmental water balance and hydrological cycle. Major applications of ET are in crop water requirement estimation, drought monitoring, crop stress assessment and irrigation scheduling.

ET can be determined by direct measurement using Lysimeter, which estimates ET over a spatial scale of ~1m and eddy covariance flux towers upto ~10-1000 m. Besides direct methods, there are many empirical and analytical methods to compute ET using meteorological data and energy fluxes. However, for operational estimation of ET at a regional scale, methodologies like the crop models or the remote sensing based technique provide a reliable alternative. Estimation of ET using the remote sensing technique uses the various geophysical and biophysical parameters collected from the satellite platform. The satellite platform enables to estimate ET over a large area, at frequent time interval with reliable accuracy levels acceptable for several applications.

Present ET estimation is based on the energy balance approach. ET is derived as a residual of the surface energy (R_n), sensible heat flux and soil heat flux. The energy balance equation is given here.

$$\lambda E = R_n - G - H$$

where λE is the latent heat flux, R_n is the net radiation, G is the soil heat flux and H is the sensible heat flux, expressed in W/m^2

Daily Actual Evapotranspiration (AET) 09 November 2020

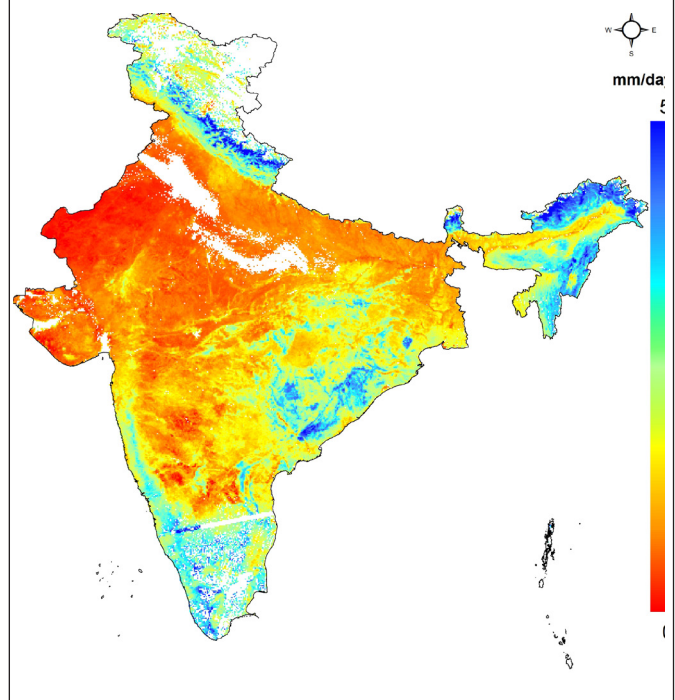


Figure 3.1: Daily Actual Evapotranspiration (AET) product generated for 9th November 2020

In this study, the Modified Priestley Taylor (PT) algorithm is used to estimate daily actual evapotranspiration. The metrological data of air temperature & dew point temperature and the satellite derived inputs like Outgoing Longwave Radiation (OLR), Insolation (INS), albedo, Normalized Difference Vegetation Index (NDVI), Land Surface Temperature (LST), cloud mask and elevation (from INSAT3D, Suomi- NPP and Cartosat 1 platform) are used

to estimate the daily AET product for clear sky condition. The critical equilibrium between the atmospheric demand for water and the constrained supply of water from the land and vegetation is derived from the satellite based LST and Vegetation Index (VI) triangle (LST-VI triangle). The warm and cold edge derived from this triangle forms the basis in the PT algorithm to estimate actual ET (AET).

The ET products are derived at $3' \times 3'$ ($\sim 5 \text{ km} \times 5 \text{ km}$) spatial resolution on daily time scale over India. Semi-automatic process chain was established for near real time product generation. Instantaneous flux value estimated is integrated to daily AET in mm/day for day length over the spatial domain. Figure 3.1 shows a sample AET product of 9th November 2020.

4. Ozone variability: Influence by its precursors and meteorological parameters - an investigation

Ozone (O_3) is a minor gas naturally present in Earth's atmosphere. About 90% of atmospheric ozone resides in the lower to middle stratosphere between about 15 and 35 km altitude which is referred to as the ozone layer while only 10% of ozone is found in the troposphere. Ground level ozone (tropospheric ozone) is identified as an Essential Climate Variable due to its significant impact on air quality and global climate system. Tropospheric ozone absorbs solar radiation in 9-10 μm range and therefore is a greenhouse gas. As compared to CO_2 on per molecule basis, O_3 has 1200–2000 times more radiative forcing.

Tropospheric ozone is a short-lived climate pollutant and is produced in-situ by photochemical reactions involving sunlight and ozone precursors species such as carbon monoxide (CO), nitrogen oxides (NO_x), hydrocarbons (e.g., methane) and non-methane volatile organic compounds and secondly through the intrusion from stratospheric altitudes through eddy diffusion or

through transport processes. The study presents the results on O_3 variability due to its precursors at sub-urban site of NRSC, Shadnagar. Also, the study focused on influence of meteorological parameters on O_3 concentrations and impact of Black Carbon (BC) on trace gases (CO and O_3). Boundary layer height (BLH) variation on ozone and BC concentrations along with long range transport on pollutants are also addressed.

During the study period, O_3 concentration was observed to be high during winter with a mean value of 35.54 ± 7.16 ppbv and low during monsoon (June-September) with a mean value of 12.70 ± 3.55 ppbv whereas the mean O_3 concentration during pre-monsoon (32.63 ± 9.96 ppbv) and post-monsoon (27.82 ± 7.94 ppbv) varied between winter and monsoon (Figure 4.1a). However, high O_3 concentration of ~ 68.0 ppbv is observed in the month of December 2014 for the entire study period. This could be due to long range transport and temperature inversion effect in boundary layer, which results in trapping of ozone near the Earth's surface. NO_x and CO showed reverse diurnal patterns with O_3 since NO_x and CO are O_3 precursors. Further, low concentrations of NO_x and CO were observed during afternoon hours where O_3 concentration reached peak value as shown in figure 4.1a.

NO_x concentration is observed to be high during pre-monsoon followed by winter, post-monsoon and monsoon during August 2014 to May 2017. Blowing winds might result in dispersion of O_3 during post-monsoon and during pre-monsoon high O_3 concentration is due to direct linear relationship with solar radiation intensity (temperature) and low relative humidity. BLH is also high during pre-monsoon, which allows the O_3 rich air to penetrate downward and increase the O_3 concentration at the study site. Mean seasonal value of CO were observed to be 201.21 ± 36.90 ppbv, 222.61 ± 37.31 ppbv, 170.14 ± 14.34 ppbv, 249.59 ± 52.03 ppbv respectively during winter, pre-monsoon, monsoon and post-monsoon during January 2016 to May 2017 as shown in figure 4.1a. High CO concentration during post-monsoon and pre-monsoon were observed, which could be due

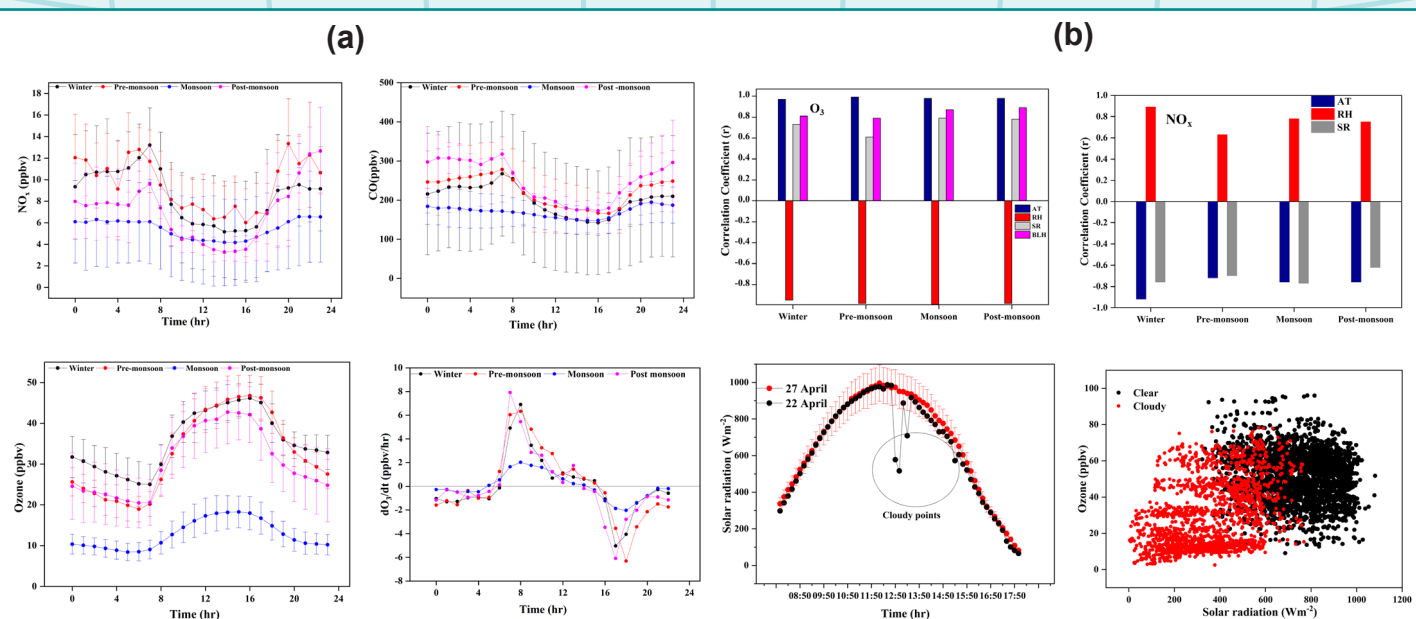


Figure 4.1: Seasonal and intra-seasonal variations of (a) O_3 , NO_x , CO, rate of change of O_3 during the study period (b) Correlation coefficient (r) of AT, RH, SR and BLH with the concentrations of O_3 , NO_x and Solar radiation on a clear and cloudy day on 27th April 2016 and 22nd April 2016 with variability of ozone concentration (ppbv) as a function of solar radiation (Wm^{-2}) during 12:00-13:50 hrs.

to long range transport of air mass containing extra pumping of CO due to biomass burning during this period. During winter and pre-monsoon, the high levels of trace gases can be due to increase in emissions from the local sources as well as long range transport from the polluted areas.

Irrespective of seasonal changes, positive and strong correlation coefficients (r) (0.97-0.99) were observed between O_3 and Air Temperature (AT) (Figure 4.1b). Photolysis efficiency is dependent on incoming radiation that controls the temperature and thus a strong positive correlation between O_3 and AT was observed.

The rate of formation of O_3 through photochemical processes depends on intensity of incoming Solar Radiation (SR) and presence of precursors. Positive correlation was observed between O_3 and SR whereas negative correlation was observed between NO_x and SR for all the seasons. Further, the correlation between O_3 and BLH were 0.81 0.79, 0.87 and 0.89 during winter, pre-monsoon, monsoon and post-monsoon respectively. Thus, the present analysis indicates that variability of O_3 is strongly influenced by meteorological parameters and levels of PCRs. The observed average values of O_3 and solar radiation were 51.40ppbv and $738.16Wm^{-2}$ during clear sky conditions and 29.49ppbv and $354.81Wm^{-2}$ respectively during cloudy conditions as shown in figure 4.1b. Increase of 42.6 % and 51.93% was observed in ozone concentration and solar radiation with respect to clear sky conditions. Hence study revealed that solar radiation is important parameter for ozone formation.

5. Changes in regional meteorology due to land use / land cover alterations

Changes in land use and land cover (LULC) affect regional meteorological conditions. Effect of such LULC changes on atmospheric parameters and surface fluxes over Northwest India are examined in the present study, using satellite observations, WRF-Solar model simulations and reanalysis data. The data set used in the study includes LULC classes from AWIFS onboard IRS-P6 (Resourcesat1) and Moderate Resolution Imaging Spectroradiometer (MODIS) onboard Aqua, along with atmospheric parameters from AIRS onboard Aqua and reanalysis data from MERRA2 and NCEP/NCAR-1. Comparison of LULC maps in 2003 and 2012 shows conversion of large areas of barren land to open shrubland and open shrubland to cropland over Northwest India. WRF-Solar simulations are carried out to quantify the effects of these LULC changes on meteorological parameters and surface fluxes. Model simulations show decrease in sensible heat flux ($-5.85 \pm 0.24Wm^{-2}$) and air temperature ($-0.14 \pm 0.005K$), along with simultaneous increase in latent heat flux ($11.03 \pm 0.41Wm^{-2}$) and relative humidity ($1.48 \pm 0.03\%$), due to the LULC alterations. AIRS measurements and MERRA2 reanalysis products also show similar changes. However, actual changes in meteorological parameters and surface fluxes are due to the combined effects of all influencing factors including LULC changes. In order to delineate the effects of LULC alterations alone, Observation Minus Reanalysis (OMR) method is used in the study. Results from OMR analysis also corroborate the model simulated changes in regional meteorology due to LULC changes. The study shows that the cooling due to LULC changes (Figure 5.1) over Northwest

India partly offsets the warming due to increase in GHGs over this region.

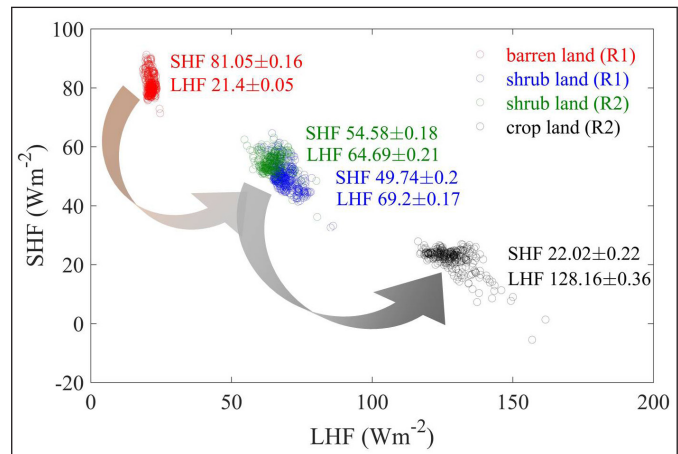


Figure 5.1: Changes in daily mean sensible heat flux and latent heat flux due to the conversion of barren land to open shrubland and open shrubland to cropland over Northwest India, from WRF-Solar model simulations

Releases



Release of P2P - July 2020



Release of Samvaad - September 2020

Dr. Raj Kumar has taken over as Director, NRSC from 1st January 2021



6. Bhuvan

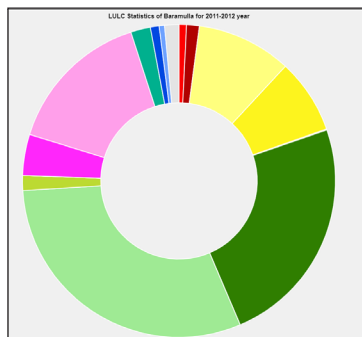
Bhuvan Application Programming Interfaces

Bhuvan, ISRO's Geoportal, provides a set of APIs for developers and users, available at <https://bhuvan-app1.nrsc.gov.in/api/>. All these APIs follow JSON or GeoJSON standards, enabling compatibility across platforms. Some of the major APIs available on Bhuvan are Maps API, States and Districts API, Geo-coding and Reverse Geo-coding API, Routing API, Land Use and Land Cover (LULC) API and Proximity API.

Geo-coding API: 'Village Geo-coding' and 'Reverse Geo-coding' APIs give user the ability to access the data on Indian villages as per 2001 Census. While Geo-coding API provides details for a given name of Village, Reverse Geo-coding API provides the details for a given location (i.e. latitude and longitude).

Proximity API: 'Proximity API' provides information on nearest hospitals and post offices with buffer defined by the user in meters.

Thematic Statistics API: 'LULC 50k Statistics API' provides the details of state-wise or district-wise statistics of LULC data for 2005-06 and 2011-12. The statistics are generated either as a JSON output or a pie chart with area information (Figure 6.1).



'LULC AOI Statistics API': Figure 6.1: Pie chart output for Bhuvan 'LULC 50k Statistics API' provides the statistics of all the LULC types present in an area of interest (AOI), which has to be given in Well Known Text (WKT) format (Figure 6.2).

LULC Class	Area (sq.km.)	Percentage (%)
Builtup,Urban	35.24	0.768
Builtup,Rural	60.69	1.323
Builtup,Mining	0.08	0.002
Agriculture,Crop land	450.46	9.818
Agriculture,Plantation	353.09	7.696
Agriculture,Fallow	5.13	0.112
Agriculture, Current Shifting Cultivation	0.0	0.000
Forest,Evergreen/ Semi evergreen	1095.71	23.882
Forest,Deciduous	0	0.000
Forest,Forest Plantation	0.0	0.000
Forest,Scrub Forest	1395.6	30.418
Forest,Swamp/ Mangroves	0.0	0.000
Grass/Grazing	70.64	1.540
Barren/unculturable/ Wastelands, Salt Affected land	0.0	0.000
Barren/unculturable/ Wastelands, Gullied/Ravinous Land	0.0	0.000
Barren/unculturable/ Wastelands, Scrub land	194.92	4.248
Barren/unculturable/ Wastelands, Sandy area	0.09	0.002
Barren/unculturable/ Wastelands, Barren rocky	698.33	15.221
Barren/unculturable/ Wastelands, Rann	0.0	0.000
Wetlands/Water Bodies, Inland Wetland	93.64	2.041
Wetlands/Water Bodies, CoastalWetland	0.0	0.000
Wetlands/Water Bodies, River/Stream/canals	41.01	0.894
Wetlands/Water Bodies, Reservoir/Lakes/Ponds	25.1	0.547
Snow and Glacier	68.26	1.488
Total Area		4588 sq.km.

Figure 6.2: Tabular statistics output for Bhuvan 'LULC 50k Statistics API'

Maps API: 'Bhuvan Maps API' is the latest addition to the set of Bhuvan APIs. Bhuvan Maps API provides users the ability to use Bhuvan Vector map in their applications. This API also allows creating popup and markers on the map. Further, with the help of Maps API, users can now get states and districts boundaries as a layer in their applications (Figure 6.3)

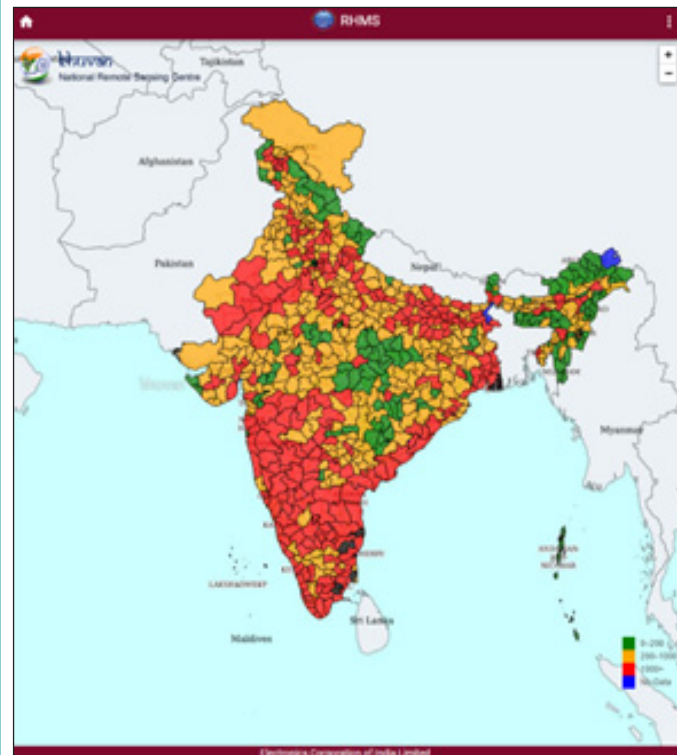


Figure 6.3: Bhuvan 'Maps and Districts APIs' in usage showing district-wise COVID statistics in ECIL Covid App

Bhuvan- NHRR mobile application, a novel approach for data collection

A unique challenge was received in the form of a project for the creation of National Health Resources Repository (NHRR), through the first ever, fully digital census of all health establishments across the nation for the Ministry of Health & Family Welfare (MoHFW), New Delhi. The census requirement stated the need for collecting 4400+ attributes through 2800+ questions asked through 11 questionnaires. Due to the paucity of time and the fact that the questionnaires were being modified dynamically as the project was being rolled out, it was difficult to create a mobile application for this purpose using the conventional methods. .

A new approach of Open Data Kit (ODK) based mobile application was created, which is a form-agnostic application. The mobile application developed through this approach acts as a container for forms that can be generated independently using excel sheets. This android based mobile (tablet) application has provided reliable user experience for collection of complex health sector data along with necessary security features (Figure 6.4).

NHRR project nationwide data collection for all health establishments is in progress. At present work is being carried out for all states (except West Bengal) with the help of 12,800 field investigators, supervisors and regional programme management units. Data of about 9.97 lakh health establishments have been collected till December 2020 from 21,50,612 enumeration blocks.

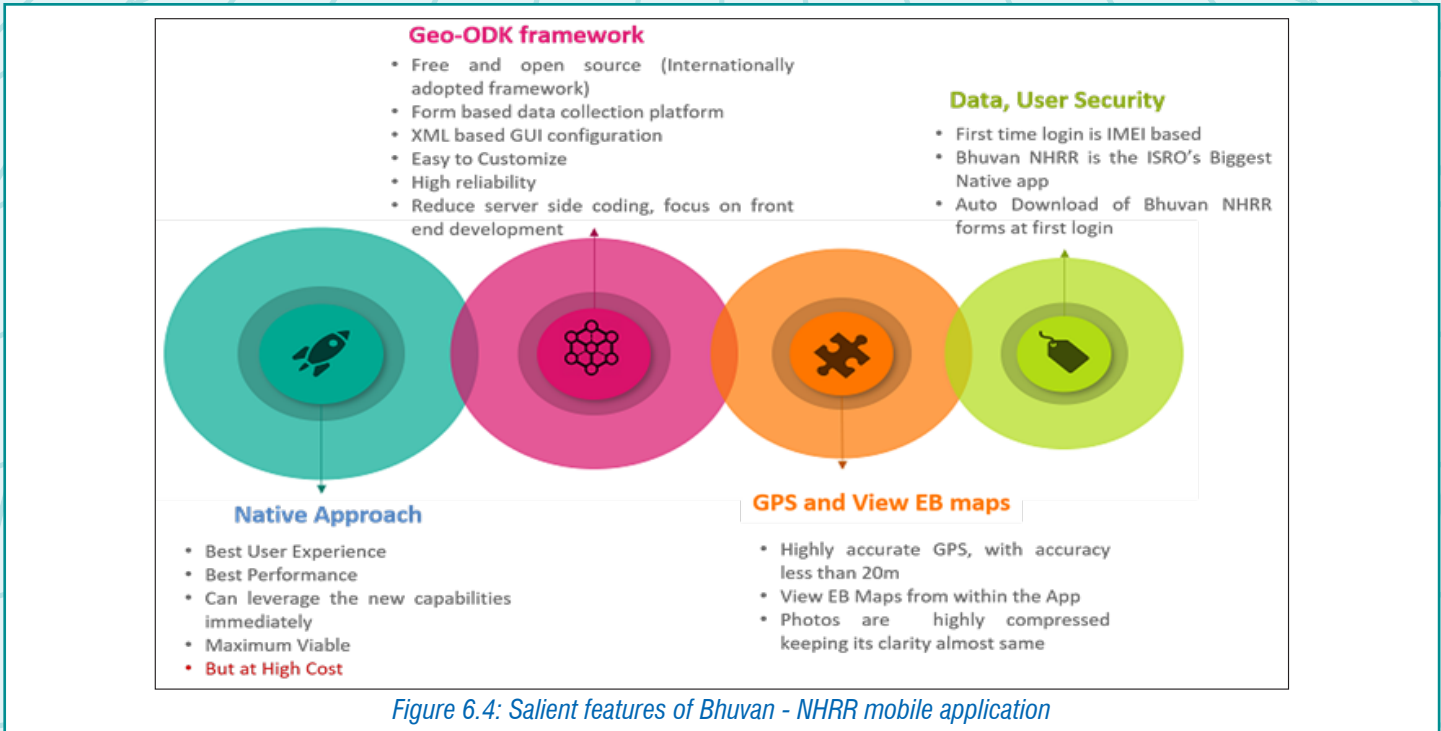


Figure 6.4: Salient features of Bhuvan - NHRR mobile application

Salient features of Bhuvan – NHRR mobile application

Sl. No.	Mobile App Development - Work Component	Technology Used
1.	Mobile app development	Android v 4.2 (min. Jellybean), Open Data Kit, XML Sforms (XML form)
2.	IDE	Android Studio, Brackets
3.	Mobile Server Programming	PHP v5.0, Java
4.	Mobile Spatial Visualization	OSMdroid
5.	Prototyping Tool	Just-in Mind
6.	Web Server Programming	Node.js v6.11.1
7.	Database	Postgre SQL v9.3, PostGIS, SQLite

7. Vicarious calibration activities augmentation for ISRO EO optical on orbit sensors using RadCalNet data

CEOS Working Group on Calibration & Validation (WGCV) has created RadCalNet (Radiometric Calibration Network), a network of well-characterized surface targets, equipped with automated instruments to allow Systeme International (d'unites) (SI) traceable radiometric Cal/Val of medium to high resolution satellite optical sensors (visible to SWIR). The automated systems of RadCalNet increase the number of potential sensor match-ups and reduces overall uncertainty. This will also help to overcome the seasons created restrictions in the periodic calibration the sensors. The goal of RadCalNet is to provide the user community with high-quality, harmonized radiometric calibration data with well-documented uncertainties.

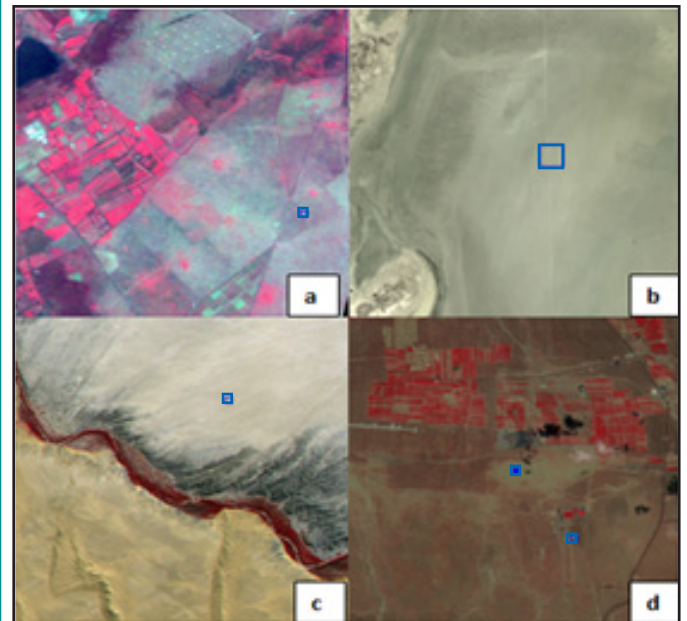
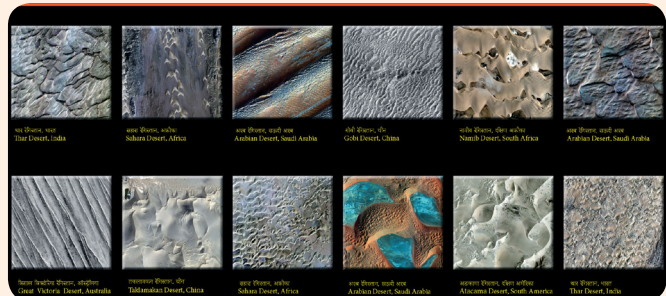


Figure 7.1: RS2/2A LISS 3 images of (a) LCFR (b) RVUS (c) GONA and (d) BTCN & BSCN sites marked in blue squares.

Release of Digital Calendar 2021



Global sand dune landscapes



The RadCalNet currently consists of five instrumented sites located in Railroad Valley (RRV) Playa in the United States (RVUS), the La Crau site in France (LCFR), the Gobabeb site in Namibia (GONA), the Baotou site (BTCN) and the Baotou Sand site (BSCN) in China. Figure 7.1 shows the location of these sites as imaged by RS2/2A-LISS3 sensor in blue squares.

Table 7.1 gives the details of the location, elevation and reflectance spectra representative area of these five sites.

Table 7.1: Geolocation, elevation and surface measurement area of RadCalNet sites

Site Name	Latitude	Longitude	Elevation	RadCalNet TOA reflectance spectra representative of
Railroad Valley	38.497°	-115.690°	1435 m	1km * 1km
La Crau	43.559°	4.864°	20 m	Disk of 30 m radius
Baotou	40.852°	109.629°	1307 m	48m * 48m
Baotou Sand	40.866°	109.615°	1295 m	NA
Gobabeb	23.600°	15.119°	510 m	Disk of 30 m radius

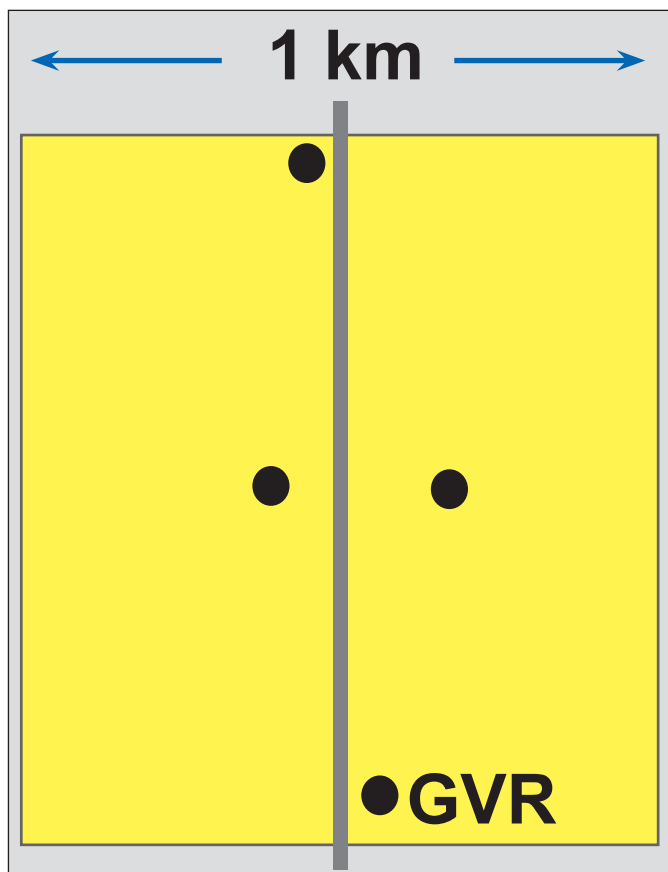


Figure 7.2: The position of four GVR in RVUS site measurement region marked in blue squares. Source: RadCalNet quick start guide

The RadCalNet provides atmospheric data along with spectrally resolved TOA (top-of-atmosphere) reflectance for a nadir view, at 30 min intervals from 9 am to 3 pm local standard time for a given site. The TOA reflectance has a spectral sampling of 10 nm intervals and covers the 400 nm to 1000 nm spectral range (required for all sites), with data for longer wavelengths (upto 2500 nm; also 10 nm intervals) provided in those cases where the site provider is capable of a broader spectral range (Figure 7.2).

An attempt was made to calibrate RS2-AWiFS 'B' by comparing the on-orbit observations of the sensor with the near-simultaneous TOA reflectance measurements from the Railroad Valley (RRV), US (RVUS) site. The RVUS site, maintained and operated by the Remote Sensing Group (RSG), University of Arizona, includes four multispectral ground viewing radiometers (GVRs) (Figure 7.2) to determine the surface reflectance in a 1 km x 1 km area as shown by the blue square in Figure 7.1(b). The site is a spatially homogenous section of dry lakebed, consisting of compacted clay-rich lacustrine deposits forming a relatively smooth surface. The deployed nadir-viewing GVRs have eight spectral channels from 400 to 1550 nm. Near-nadir overpasses of AWiFS-B sensor for the year 2019 are processed and matched up with near-simultaneous RadCalNet measurements. The AWiFS-B sensor covers RVP site in the following path/rows: 252/41, 253/41, 254/41 and 255/41. There were 11 cloud free matchups for the AWiFS sensor centered over the RVP site. TOA reflectance were calculated for ~1 km X 1 km area centred at the RVUS site geolocation, which corresponds to approximately 17 X 17 pixels. The simulated RadCalNet TOA reflectance provided at 10 nm spectral resolution were interpolated to 1 nm resolution and then convolved with respective spectral response function of each band to make the companions with the measured TOA reflectance. Since RadCalNet provides data every 30 min interval, the nearest matchup in time was used to generate the per band TOA reflectance. The mean ratio of satellite measured TOA reflectance to the RadCalNet simulated TOA in different bands of AWiFS sensor for year 2019 (11 images) are plotted in Figure 7.3

The largest deviations were observed for the SWIR band (B5) with a mean ratio of 0.86. The red (B3) and NIR (B4) had very close agreement with RadCalNet simulated value with ratios mostly falling in range 0.97-1.01. For the green band (B2) the ratios were slightly on the higher side with ratio increasing to 1.1. The calibration results over RVP site indicate slight deviation for the SWIR band of AWiFS sensor. The rest of the bands of the sensors are performing well and shows an agreement within 10%.

The observed results are concurrent with the Indian wide field calibration site of Rajasthan. Currently, this facility is used in campaign mode annually. This augmented facility will ensure to assess the traceability of sensors more frequently as the ground data is made available through CEOS portal.

Bhoonidhi

Bhoonidhi - a regional data hub for IRS, the Sentinel satellites series and Landsat-8 OLI data. The portal can be accessed at <https://bhoonidhi.nrsc.gov.in>



Bhoonidhi
ISRO's Open Data Access

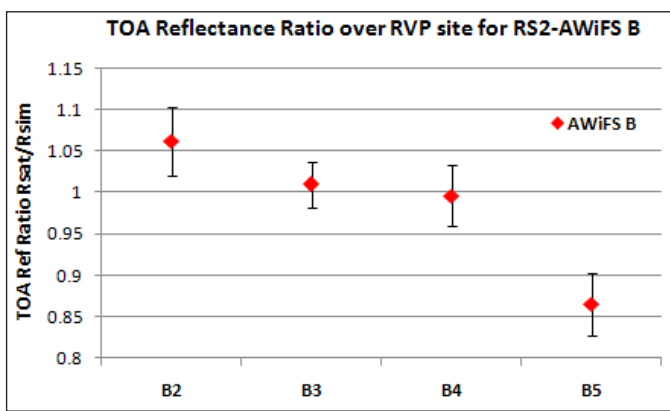


Figure 7.3: Ratio between observed and RadCalNet simulated TOA reflectance for the different bands of the AWiFS B sensor for 2019

8. Applications Validation of ICESat-2 Photon Data

NASA's Ice, Cloud, and Land Elevation Satellite-2 (ICESat-2) is a continuation to the mission targeted for studying the Earth's polar region based on operation principles of LiDAR technology. Launched in 2018, the applications of ICESat-2 were proposed to extend to other landforms as the data from it is acquired over all surface types like oceans, land, vegetation, and inland water-bodies. The specialty of ICESat-2 is that it hosts a photon counting technology supported by the Advanced Topographic Laser Altimeter System (ATLAS) instrument. The ATLAS instrument transmits a green (532 nm) laser pulses at 10 kHz and the spacecraft velocity from the ICESAT-2 nominal ~500 km yields one transmitted laser pulse every 70 cm along track. The time delay between each laser pulse from the satellite and the detected reflection from the Earth's surface is used to compute the range, and from this range the height above a reference ellipsoid is derived. ATLAS sensor produces three pairs of beams each consisting of a strong and a weak signal beam. The beam pairs are separated by 3.3 km in the cross-track direction and the distance between the strong and weak beam in the pair is 90 m. The data acquired by the ICESat-2 contains a collection of geolocated photons representing the surface height detected by the ATLAS sensor. ICESat-2 geolocated data is tested for following activities / products.

Evaluation of best-fit terrain elevation of ICESat-2 ATL08 using DGPS surveyed points: Higher-level data products of ICESat-2 like ATL08 uses an iterative filtering approach of the signal photons for capturing canopy height and terrain height. Process of evaluation has been accomplished on the best-fit elevation granules on the land parts with DGPS surveyed points. 40 points were surveyed for elevation in the semi-arid region with different topographies with varied surface cover. Mean bias error computed from the best-fit elevation from ICESat-2 ATL08 data product and corresponding DGPS surveyed points is close to zero. The conformity between these two sets of elevation values is less than 40 cm (RMSE).

Validation of ICESat-2 Surface Water Level Product ATL13 with Near Real Time Gauge Data: From the Level 2 master product called ATL03 numerous sub-data product are generated and are made available to the public through the National Snow and Ice

Data Center. One of the products namely ATL13 is a specialized geophysical data product that gives along-track and near-shore water surface height distribution within the water masks. ATL13 data product are validated with 46 observations made with near real-time gauged data for 15 reservoirs/water bodies. The maximum uncertainty observed for this data product is at centimeter-level.

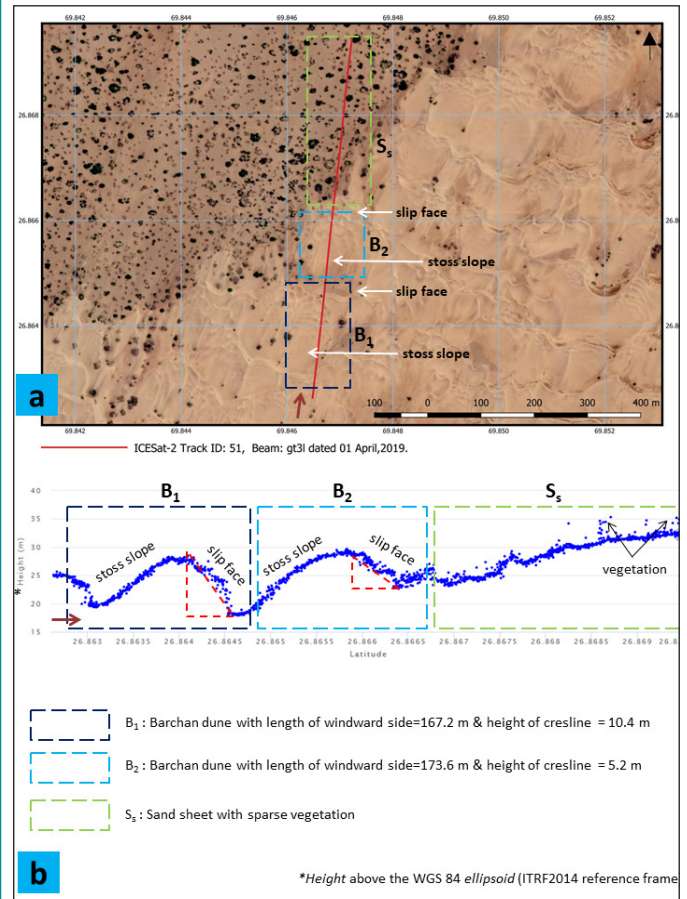


Figure 8.1: Morphological profile generated from ICESat-2 photon counting data over an area containing barchans and dunes and sand sheet with sparse vegetation

Morphological characterisation of sand dunes using altimeter data: Aeolian process leads to the transportation and accumulation of sand particles that result in sand dune landforms. Here, 2D profiles generated from the beams of ICESat-2 ground-tracks acquired over sand dunes of the Thar Desert region were analysed for detecting the geomorphological parameters. Observations from the cross-section profiles have resulted in giving unprecedented details about the shapes and morphological settings of various barchanoids, compound sand dunes, parabolic, longitudinal, and transverse dunes. Morphological parameters of sand dunes like the length of the stoss slope, crest height, slip face details, inter-arms spacing, height of the trailing arms, length of the depositional lobes, and sinuosity of the recurring crest lines were retrieved with ease from the Level-2A data product namely ATL03.

Applications of ICESat-2 altimeter data for urban morphological studies: Urban morphology is the study of urban form and deals with the size, shapes, and dimensions of the building blocks that make the urban landscapes. Retrieval of building height is an important parameter to study the urban surface geometry; which in turn plays a pivotal role in various applications like investigating the phenomenon like urban heat islands, generation of urban

canopy layer, estimation of the urban energy balance, and urban climate change. Earlier, researchers have used the mean height of the buildings in the urban landscape to estimate the urban canopy layer and have used to study the circulation of mean airflow in the cities. Here, attempts are made to retrieve urban morphological parameters like size, density and pattern from the ICESat-2 profiles (Figure 8.2).

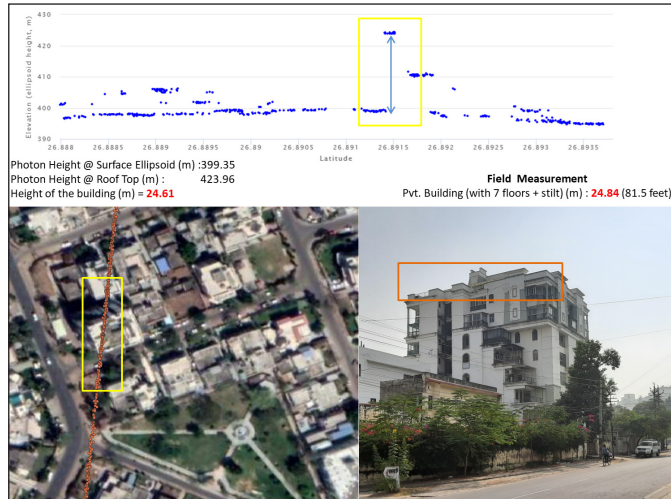


Figure 8.2: Building height extraction and evaluation with field level measurements.

9. Estimation of brine concentration in salt pans using geospatial technology

India is the third-largest salt producing country in the world with an average annual production of about 300 lakh tonnes during 2019. Gujarat is the largest salt producing state and contributes to three-fourth of the total salt production in India. Salt comes from two main sources: sea water and the sodium chloride mineral halite (also known as rock salt). Salt evaporation ponds, or salt pans, are a series of shallow artificial ponds located close to the sea and designed to extract salts from sea water through progressive evaporation. The Salt Water Concentration (density) in each pond is measured manually by sampling with Hydrometer (Baume degrees oBé) and is continuously monitored through extensive field visits. Sea water has density of 3.5oBé and Sodium Chloride crystallizes in the density range of 25 to 29 oBé. The brine density is monitored in all the salt ponds for progressive transfer of brine solution and for final transfer to factory for salt production.

The present study has been carried out to develop methodology for automation of the process of measuring brine concentration in a fast and efficient manner using satellite data. The study region is Charkala salt ponds located in Mithapur, Devbhumi Dwarka district, Gujarat (Figure 9.1), which has a desert climate with average rainfall of 393 mm. Generally, the evaporation is very high when compared to actual precipitation. Atmospherically corrected Level-2A Sentinel-2 data product was used for the analysis. Two methods, viz., a) Salinity Index Method (SIM) and b) Spectra matching method have been used. In SIM, the brine concentration was calculated using Normalized Difference Salinity Index (NDSI) and for the spectra matching method, spectra from satellite image was matched with reference spectra (Spectral Library) using Spectra Feature Fitting Method.

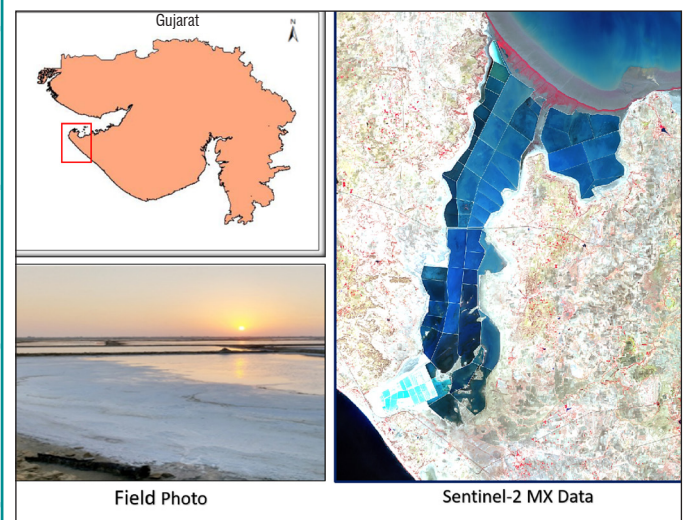


Figure 9.1: Study area and satellite image of Mithapur Devbhumi Dwarka district, Gujarat

The spectral library for about 150 spectra was generated with the help of image-derived spectra for different brine concentrations associated with corresponding field data during the same date and time of satellite pass. Pond-wise brine concentration corresponding to the satellite pass over the salt pans along with coordinates of sampling locations were provided by user organization (Figure 9.2).

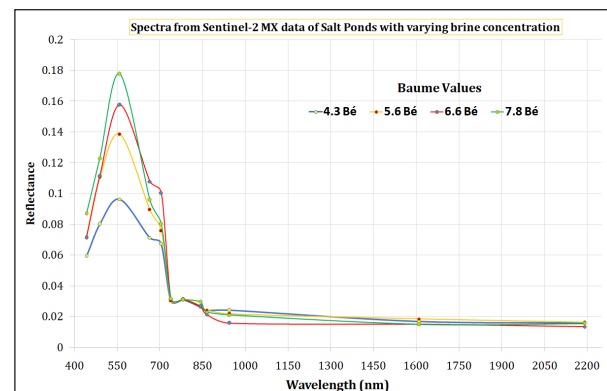


Figure 9.2: Satellite-data based reflectance for varying brine concentration (Baume Value)

The results from NDSI method and spectra matching methods showed good correlation between field-measured and satellite data-derived values with correlation ranging from 0.40 – 0.70. The results indicated an overall accuracy of ± 1.0 Baume degree for 70% of the predicted values of varying brine concentrations. To improve accuracy of the model and to collect field information, the project team carried out ground-based hyperspectral measurements using portable Spectroradiometer (350-2500 nm) during December 2019 for all series of salt ponds to validate the spectral response pattern under varying brine concentration. Further analysis is being continued by user agency, using both the methods and corresponding field values to stabilize the regression model and to fine-tune the model with weather parameters.

Cartosat-3 data products

NRSC is pleased to announce the availability of the Cartosat-3 Standard data products to the user community. Contact NDC/NRSC at data@nrsc.gov.in.



10. Real-time operational spatial flood early warning system for Tapi and Godavari rivers

Flood causes severe damage to life and properties every year all over the world. India is one of the most flood vulnerable countries in the world. During the last decade, the frequency of floods in India has increased causing large scale damages. Development of medium range spatial flood early warning models for large catchments is a challenging task to hydrologists. Considering the requirements at national level, spatial flood forecast models for the Godavari and Tapi rivers using space based inputs under National Hydrology Project (NHP) have been developed. The developed models are calibrated and validated thoroughly using historic discharge and rainfall data obtained from Central Water Commission and Indian Meteorological Department (IMD), respectively. Spatial flood early warning models for major floodplains of these two rivers are developed using high resolution digital terrain models from ALTM. Models are being run in near-real time for the year 2020 (June to October) using near-real-time rainfall data and rainfall forecast data obtained from IMD and WRF/GEFS model. Flood alerts were disseminated through NHP portal and Bhuvan Geo-portals.

Accuracy of flood discharge forecast estimated using inundation simulation is found to be more than 80%. Godavari flood alerts were also given to Andhra Pradesh State Disaster Management Authority (APSDMA) during floods in Godavari River in 2020. This helped relief and rescue operations during floods, flood disaster risk reduction, and flood disaster management. Flood forecast hydrographs of Godavari and Tapi rivers are shown in Figures 10.1 & 10.2, respectively, and spatial flood inundation simulation in Godavari is shown in Figure 10.3.

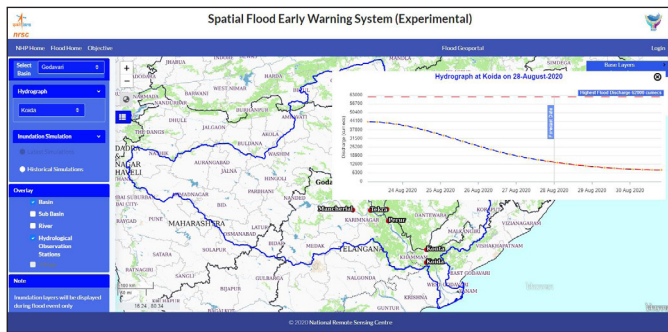


Figure 10.1: Flood Hydrograph at Koida in Godavari river (Aug 2020)

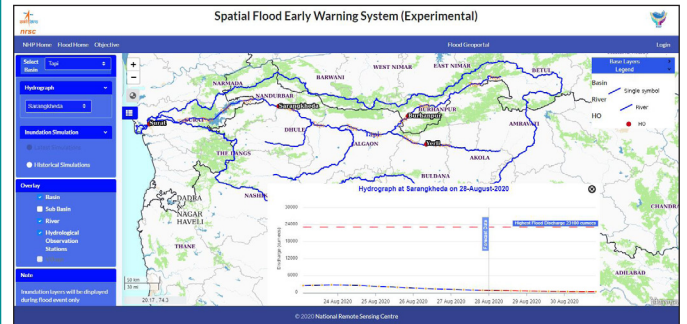


Figure 10.2: Flood Forecast Hydrograph at Sarangkhedha in Tapi river (Aug 2020)

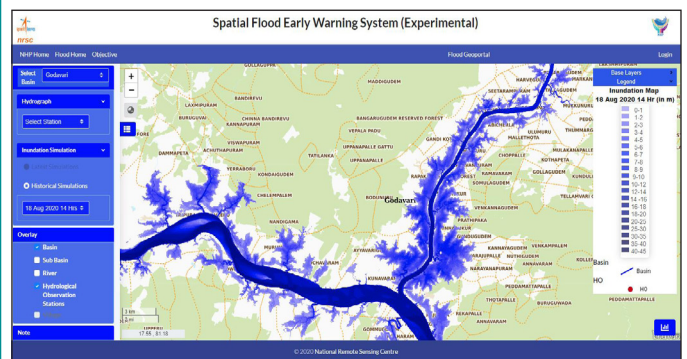
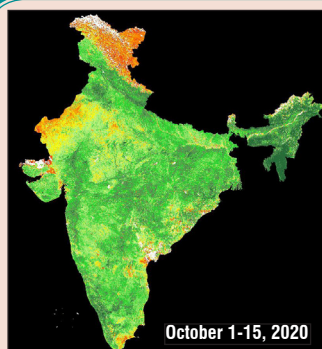


Figure 10.3: Flood Inundation Simulation for Godavari river (18 Aug 2020)

NYAYA VIKAS v2.0 launch and Capacity Building

‘NYAYA VIKAS’ is an online monitoring tool for monitoring the physical and financial progress of Judicial infrastructure at national level. Nyaya Vikas v2.0 with enhanced features and mobile application compatible to android and iOS platforms was launched on 1st April, 2020. Capacity building was conducted in June 2020 through video conference for officials of States/UTs.



Satellite data products

- Generated and archived more than 2.85 lakh products in six months.
- Improved accuracy of high resolution products through monostrip modelling.
- Generated more than 4000 value added products for Integrated Watershed Management Programme (IWMP)
- Fortnightly NDVI products generated for MNCFC, New Delhi

11. Locust surveillance using geospatial technology

Cyclones like Sagar, Mekunu and Luban brought heavy rains in the empty quarter of the Arabian Peninsula during the year 2018, and have favored the ecological conditions to exacerbate the desert locust outbreaks. The situation of locust swarm migration has been intensified during Amphan cyclone in the Bay of Bengal and led the trajectories of migration to most parts of the countries. Effective utilization of multi-platform and multi-sensor satellite data from various open source platforms like MOSDAC, Bhuvan and

others was done to release 12 weekly, 2 fortnightly and 1 monthly bulletin comprising of:

- Heuristic prediction of locust swarm trajectory based on vegetation status, wind parameters and existing geolocations of locust swarms.
- Maps of wind parameters (speed and direction), soil moisture (root zone and sub-surface), accumulated rainfall, land surface temperature, FCC, NDVI data and etc.
- Story / Locust impact / crop loss analysis during the bulletin period
- Knowledge base (like climate and locust relation, understanding the locust behavior and life cycle events, etc.)

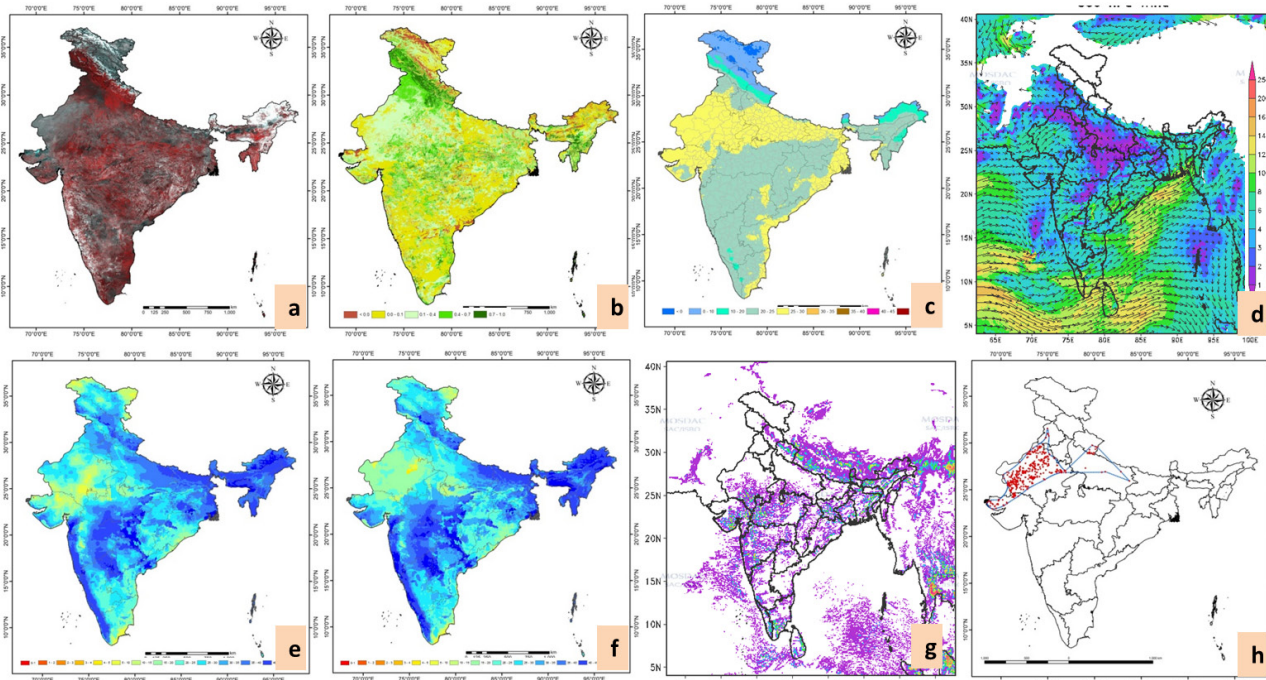


Figure 11.1: Integrated set of various remote sensing data used for heuristic prediction of Locust and to generate Locust threat maps. (a) False color composite, (b) NDVI, (c) LST, (d) Wind vectors, (e) Surface soil moisture, (f) Root-zone soil moisture, (g) accumulated rainfall, (h) points of existing Locust provided by LWO/FAO

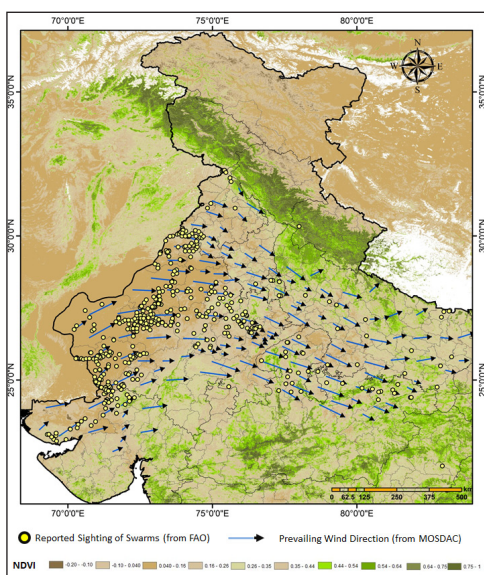


Figure 11.2: Heuristic prediction model with inputs like vegetation status, wind parameters and existing locust swarms provided by LWO

A dedicated web portal titled 'Bhuvan-Locust' and mobile app titled 'Bhuvan-Tiddi' has also been designed and developed which is ready for hosting on Bhuvan Regional Node. The information is being used by Locust Warning Organization, Jodhpur.

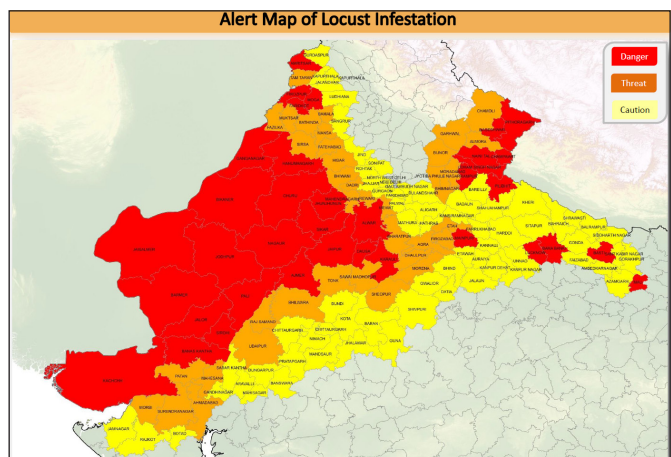


Figure 11.3: Alert map of locust infestation



12. Monitoring of net primary productivity of cotton agroecosystem in central India using remote sensing-based models

Monitoring of carbon dynamics is a crucial issue in the study of global climate change. Vegetation plays an important role in the carbon cycle as photosynthesis consumes and respiration produces considerable amounts of CO₂, the predominant greenhouse gas in global warming. Net Primary Productivity (NPP) is the rate at which plants accumulate carbon from the atmosphere, and is equal to the difference between carbon gained by photosynthesis, and carbon lost through plant respiration. It is commonly expressed as carbon per unit land area per unit time. NPP has been used as a key indicator to understand carbon dynamic at regional/local scale with reference to climate change perspective. Most of the studies on NPP have been concentrated on natural vegetation with very little attempt for agricultural vegetation. Given the obvious differences in NPP responses between natural and agricultural vegetation, it is essential to study agricultural NPP, particularly for countries like India, where, it is the major land use. The objective of the present study is a comparative analysis of different satellite-based models for the estimation of net primary productivity of cotton agroecosystem of the Central Indian region.

The cotton crop area of Nagpur district was estimated as 1,32,213 hectare in 2019-20 season from multitemporal IRS P6 LISS-III data using random forest classifier with overall accuracy 85% (Figure 12.1).

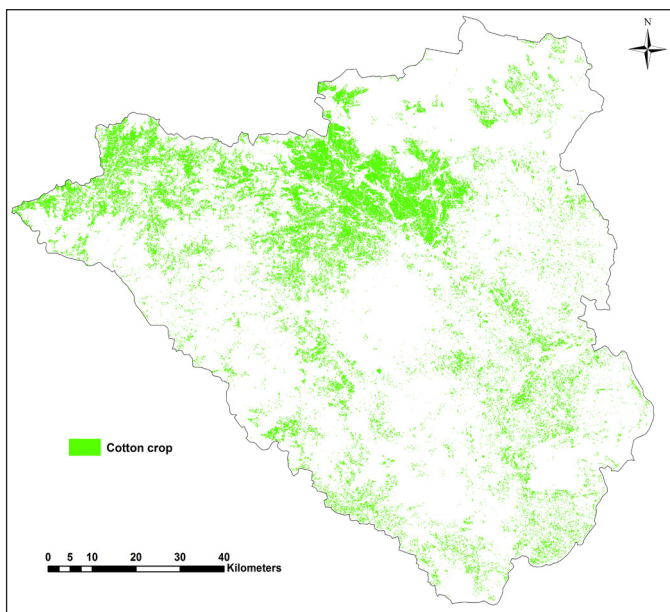


Figure 12.1: Spatial distribution of cotton crop in Nagpur district during 2019-20

NPP of cotton agroecosystem was calculated (Figure 12.2) using remote sensing-based Vegetation Photosynthesis Model (VPM), MODIS algorithm and Greenness and Radiation (GR) models. IRS P6 LISS-III, Landsat OLI & Sentinel-2 data were used in these models along with flux tower weather data.

The higher value of NPP estimated by VPM model might be due to more number of local weather parameters (cardinal temperature and atmospheric water vapor content etc.) incorporated in VPM model.

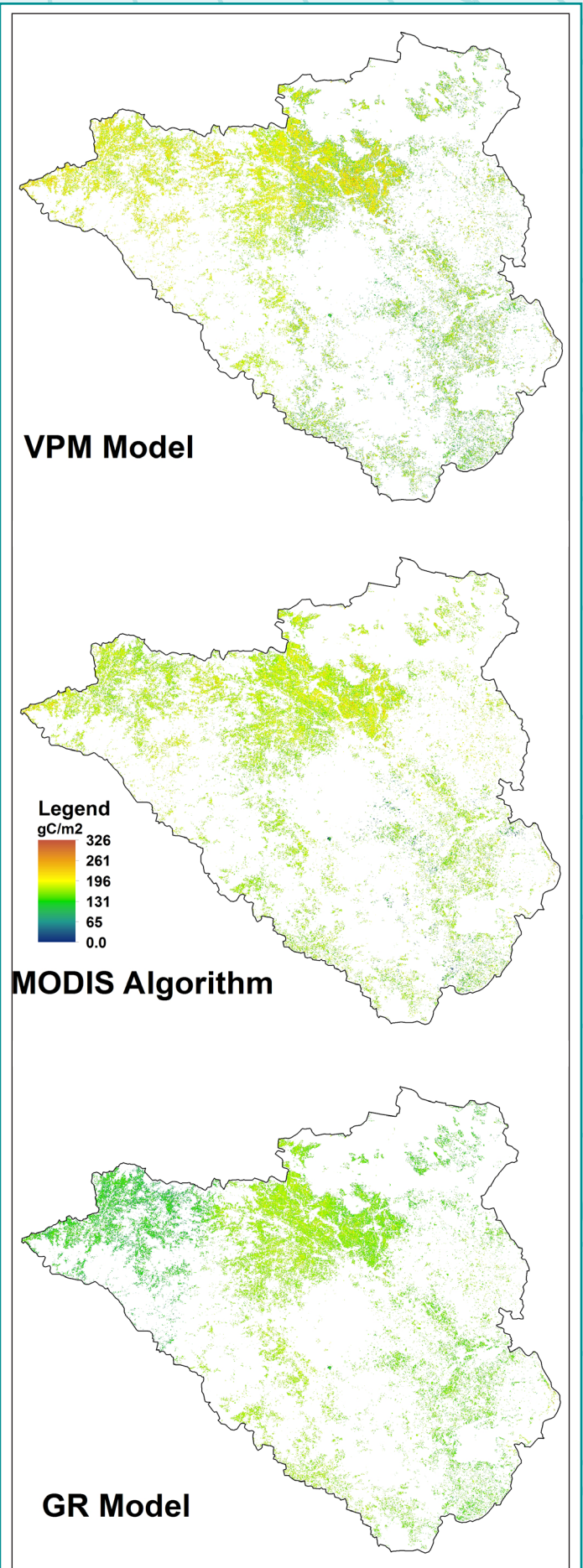


Figure 12.2: Spatial variation of NPP of cotton crop in Nagpur district during 2019-20

Table 12.1: The accumulated NPP by cotton crop (Nagpur district during 2019-20)

Model	Max NPP (gC/m ²)	Mean NPP (gC/m ²)	Accumulated NPP Tonnes of C
VPM	326	0.057	192587
MODIS	240	0.053	164836
GR Model	203	0.046	144573

Validation of the NPP estimate from different remote sensing models has been done with NRSC Eddy covariance tower situated in Cotton agroecosystem, Nagpur. Eddy covariance technique is a key atmospheric measurement technique to measure and calculate vertical turbulent fluxes within atmospheric boundary layers. The method analyzes high-frequency wind and scalar atmospheric data series, gas, energy, and momentum, which yields values of fluxes of these properties. The validation of model derived NPP with flux data estimated NPP shows that VPM model provides a better result with a coefficient of determination of 0.92. MODIS algorithm and GR models registered coefficient of determination

of 0.87 and 0.83 respectively (Figure 12.3). The results of the present study indicate the utility of satellite-based models in the estimation of NPP of different agroecosystem.

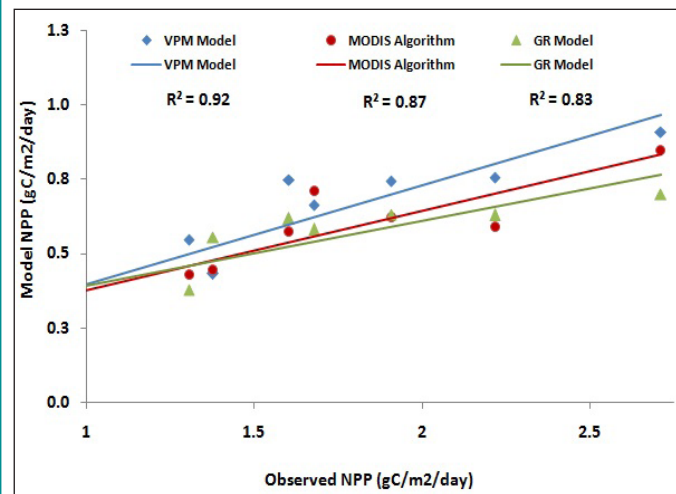


Figure 12.3: Comparative analysis and validation of models

13: SUFALAM: Development of methodology for mapping of Maize and Bajra crops grown in kharif season

ISRO has developed 15 operational field and horticultural crops mapping techniques based on satellite remote sensing and transferred to MNCFC (Mahalanobis National Crop Forecast Centre) under FASAL (Forecasting Agricultural output using Space, Agro-meteorology and Land-based observations) and CHAMAN (Coordinated Horticultural Assessment and Management using Geoinformatics) programs. ISRO has proposed to develop techniques for 10 more crops, that include short duration Kharif crops (Soybean, Maize, Bajra & Groundnut), long duration Kharif crops (Castor&Red gram) and rabi crops (Maize, Cumin, Groundnut&Mentha) under the SUFALAM project (Space Technology Utilization for Food Security, Agricultural Assessment and Monitoring).

Under SUFALAM project, development of suitable methodology for mapping of Maize and Bajra crops grown in Kharif season using temporal SAR data and Random forest Machine Learning Algorithm was taken up. Random Forest Classifier is an ensemble classifier, which makes use of several independent decision trees to classify the temporal pre-processed stacked images. Estimation of crop area for Kharif Maize (17 Districts of Uttar Pradesh) and Bajra (13 Districts of Uttar Pradesh) during 2019 was carried out using temporal SAR data (Sentinel – 1 A/B). Location map of the study area is given as Figure 13.1. Temporal backscatter profile of different crops grown in the study area is generated to understand the phenology of crops (Figure 13.2). Spatial distribution of Maize and Bajra grown during kharif season of 2019 is shown in figures 13.3 & 13.4. Mapping accuracy ranges between 60-80% and nearly 3156 ground truth points were collected for target and non-target crops from 8 districts of UP during Kharif season 2020.

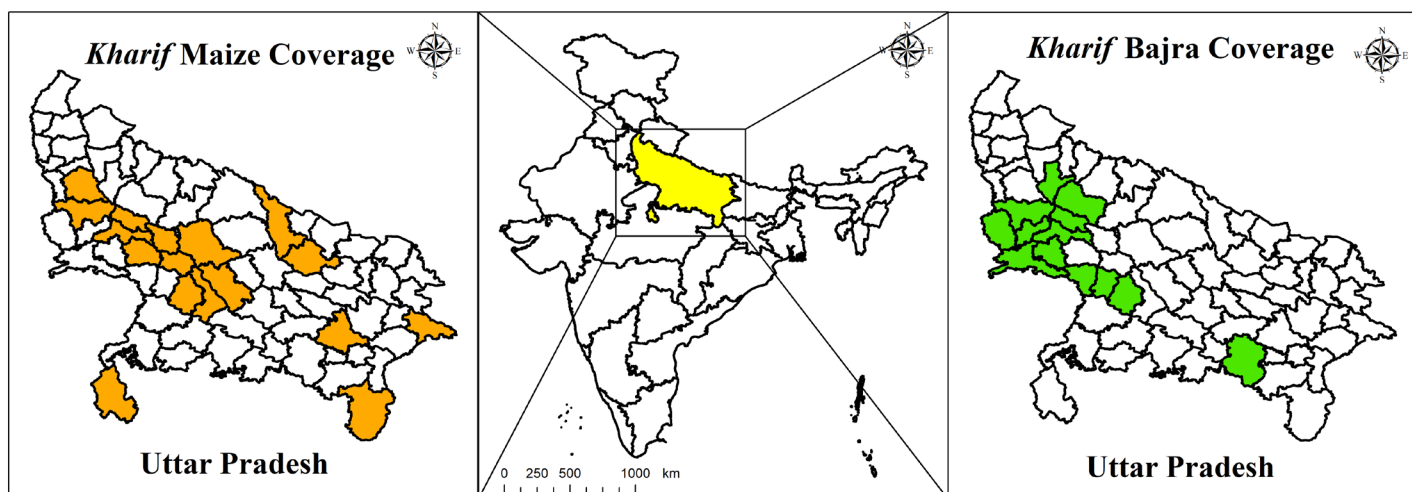


Figure 13.1: Location map of the study area

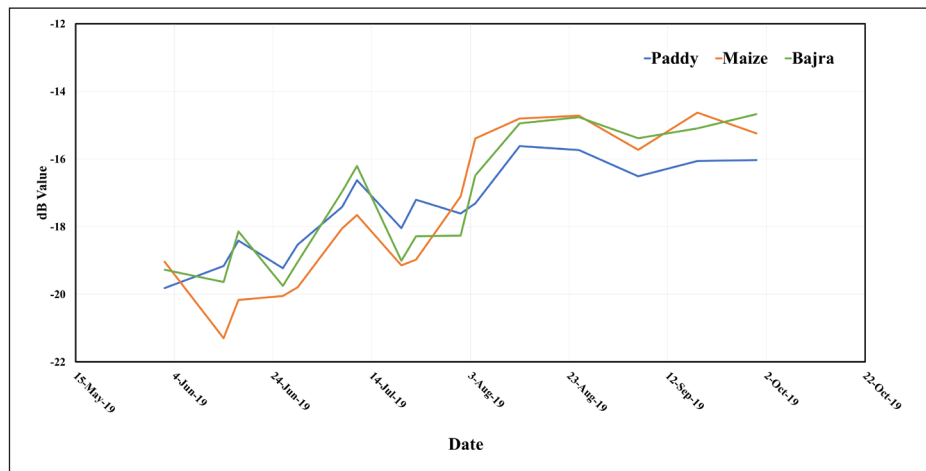


Figure 13.2 : Temporal backscatter of different crops using Sentinel 1A (VH polarization)

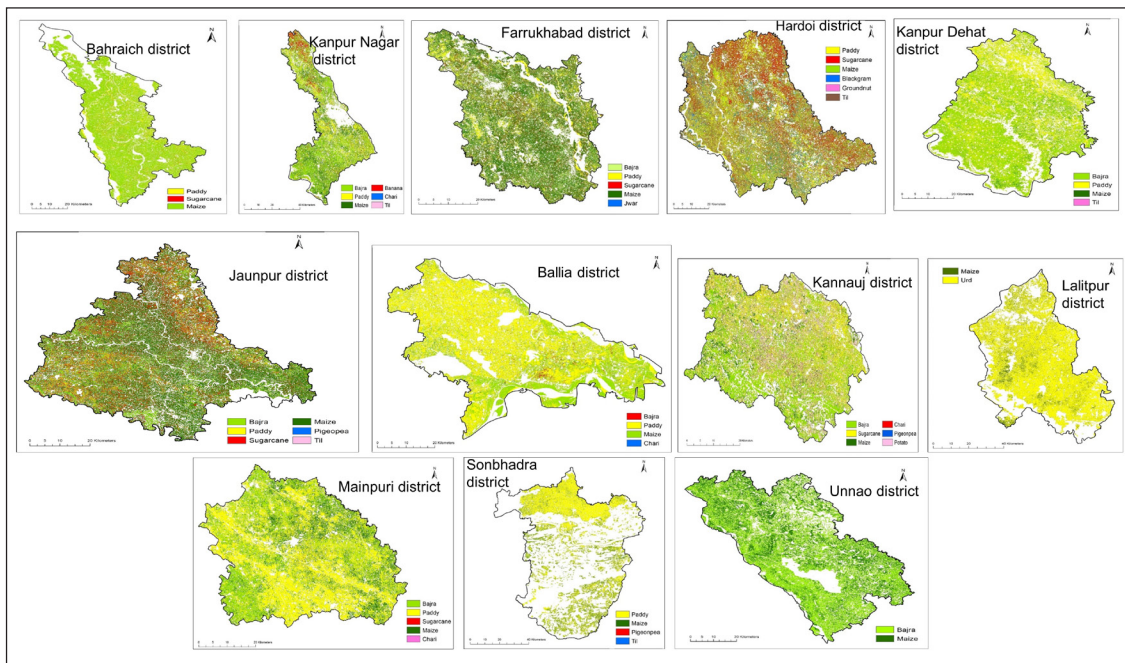


Figure 13.3: Spatial distribution of Kharif maize crop using RF classifier

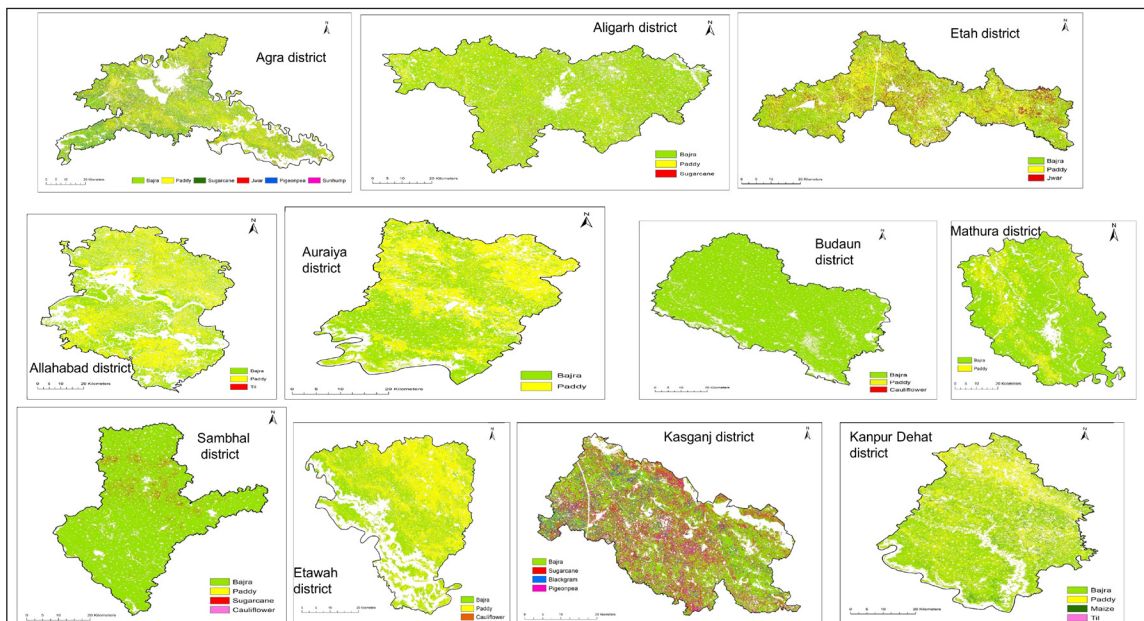


Figure 13.4: Spatial distribution of Kharif bajra crop using RF classifier

ISO 9001:2015 Lead Auditor Training Program at NRSC

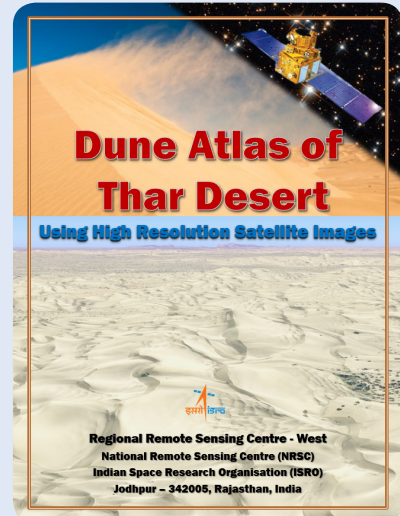
Seventh batch of Certified Lead Auditor training program was organised during 05 - 09 October, 2020 and was conducted by M/s Bureau Veritas India private limited - Hyderabad. Total 20 participants learnt about auditor's role to plan, lead and follow-up on a management system audit in accordance with ISO standards and understand/learn how to lead an audit and audit team.



Presently about 137 staff members of NRSC are trained and certified as lead auditors in ISO 9001: 2015.

Dune Atlas of Thar Desert Using High Resolution Satellite Images

The 'Dune Atlas of Thar Desert using High Resolution Satellite Images' is a comprehensive publication, which gives detailed information of dune formation with their spatial distribution in Thar Desert area. Morphometric analysis of different dune features, their types, geometry and dune dynamics were done using high resolution satellite data of IRS LISS-IV (2020), Carto merged NCC (2016) and Carto DEM (2015-16). This atlas is a useful reference document for different user community. The atlas was released by the Director, NRSC on 24th December, 2020 in virtual mode.



14. Classification of mangroves and mapping their health spatially using HysIS data

Mangrove forests or mangals are a type of intertidal wetland ecosystems. These forests grow in harsh environmental conditions with high levels of salinity, high temperature, extreme tides, high rates of sedimentation and muddy anaerobic soils. Presently, Sundarban biosphere reserve has about 26 true mangrove species, 29 mangrove associates and 29 back mangrove species belonging to 60 genera and 40 species. The objectives of the present work were to classify the mangroves into floristic composition classes and determine the health status of these spatially using Hyperspectral Imaging Satellite (HysIS) data.

The study area included the pristine mangrove habitats of Lothian Island, parts of Bhagabatpur and Dakshin Chandanpiri with neighboring land covers of Sundarbans, West Bengal. The area also harbours both diverse as well as homogenous patches of different mangrove communities. Figure 14.1 shows the index map of the study area.

HysIS data acquired on 11th December 2018 were used in the study. The data was pre-processed and atmospherically corrected using Fast Line-of-sight Atmospheric Analysis of Hypercubes (FLAASH). The data had 316 (60 visible and near infrared bands and 256 shortwave near infrared bands) bands out of which 178 bands were finally used.

Five vegetation/ spectral indices namely, Mangrove Probability Vegetation Index (MPVI) Normalized Difference Wetland Vegetation Index (NDWVI) Shortwave Infrared Absorption Depth (SIAD) Normalized Difference Infrared Index (NDII) and Atmospherically Resistant Vegetation Index (ARVI) were used for enhancing the mangroves from other/ adjoining land covers. The values of the indices were used as inputs in Decision Tree (DT) classifier. The

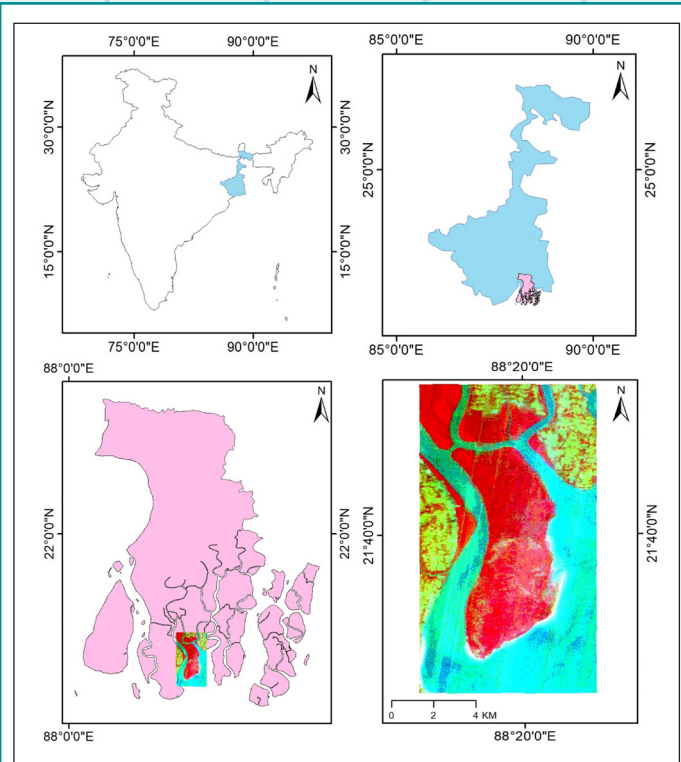


Figure 14.1: Index map of the study area and false colour composite of the HysIS data

images of the indices were stacked for highlighting the mangrove forests and DT rules for the identification of the forests were obtained after thresholding (Figure 14.2) to cover all mangrove pixels. A mangrove mask was built using the classified output of DT (Figure 14.2). Known locations of definite floristic composition and land covers were used as training site pixels.

Nine mangrove classes were obtained in the study. The classes, their compositions and classification-levels are given in Table 14.1. The classified image of the mangrove forests/ mangroves

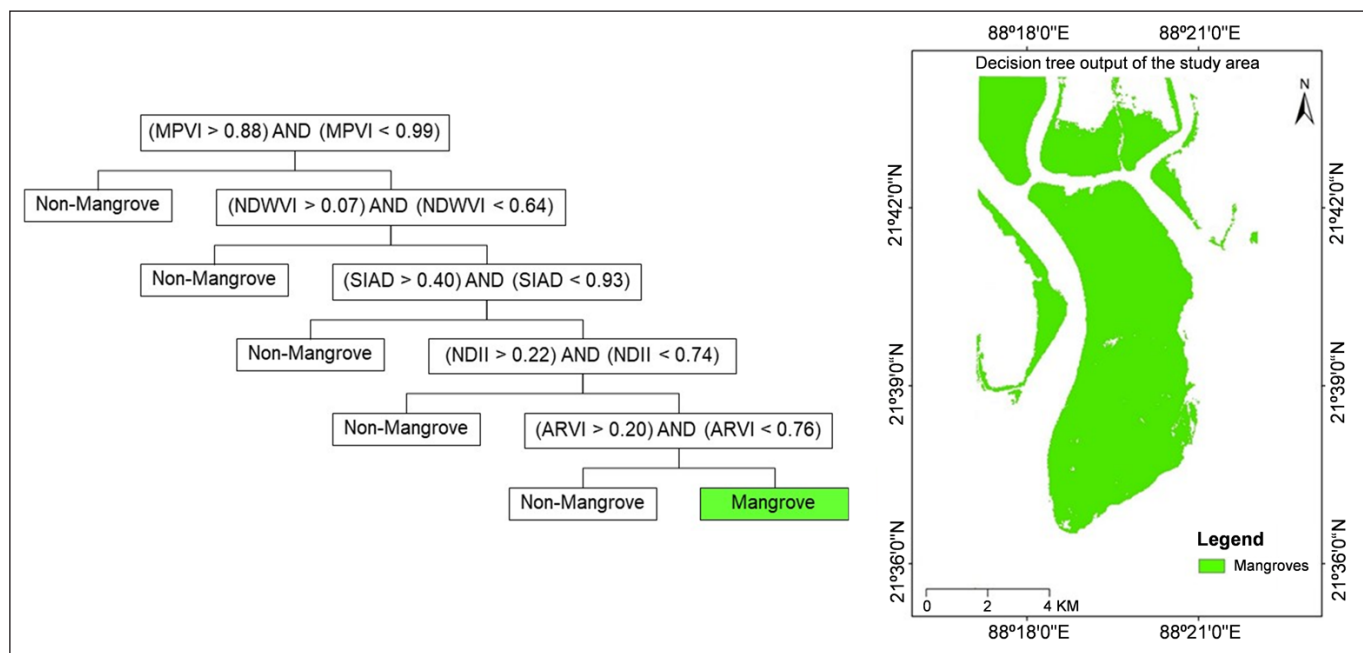


Figure 14.2: Rules for identifying mangroves in the study area using DT and DT output exhibiting the mangroves

is shown in Figure 14.3. Based on ground truth check, the overall classification accuracy achieved was 84.05% with a Kappa coefficient (K) of 0.82.

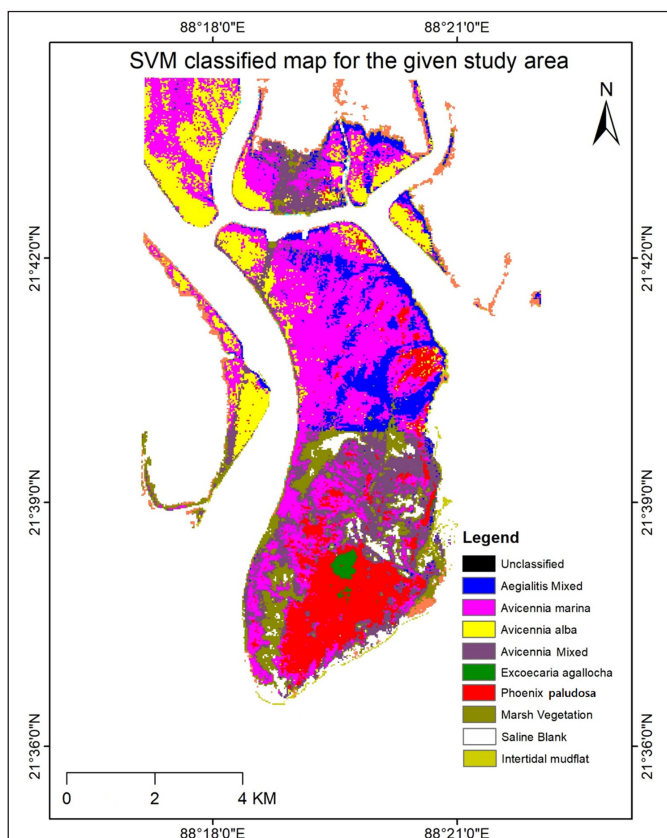


Figure 14.3: SVM classified output over the mangrove forests in the study area

The HysIS data was also used to determine the biochemical and biophysical parameters of the mangrove communities and species to detect the most-healthy, moderately healthy and less healthy or stressed mangroves. Enhanced Vegetation Index (EVI) and Vogelmann Red Edge Index 1 (VREI1) were used to

determine greenness while NDII gave moisture status of mangrove canopy. Photochemical Reflectance Index (PRI) was used as the representative of light-use efficiency of the species and communities. Carotenoid Reflectance Index 1 (CRI1) and Modified Chlorophyll Absorption Ratio Index (MCARI) were applied to exhibit the status of pigment contents in the leaves of the canopies. Additionally, VREI1 and CRI1 measured stress in vegetation.

The six health determination indices were extracted by using the mangrove mask obtained from the DT output for extracting mangrove forests. The ranges of the six vegetation indices were used in DT algorithm (Figure 14.4) to obtain the health classes for the mangrove classes (communities/ species). The result of DT algorithm indicated that the proposed indices could appreciably detect the health of the mangroves spatially. Figure 14.4 also depicts the proportion of the health status for each of the mangrove classes (excluding marsh vegetation, saline blank and intertidal mudflat).

The methodology presented in this study is being extended for other islands and localities of Indian Sundarbans and holds good opportunity to be applied to other mangrove forests for producing mangrove health maps using hyperspectral image data.

Awards

Book "Antariksh ek khoj" written by Dr. Rajashree Bothale & published by Scientific Publishers, Jodhpur has been awarded Second Prize in Delhi book fare 2020 under reference book in Hindi category by the Federation of Indian Publishers.

Mr. P V S S N Gopala Krishna, received award for best paper published in ISRS journal for the year 2019. It is titled: "Dense DSM and DTM point cloud generation using CARTOSAT-2E satellite images for high-resolution applications", Journal of the Indian Society of Remote Sensing 47, 2085-2096 (December, 2019). <https://doi.org/10.1007/s12524-019-01051-0>.

Table 14.1: Mangrove classes, class compositions and classification-levels of the mangrove classes

Mangrove class	Class composition	Classification-level
<i>Avicennia alba</i>	Pure, homogeneous and dense stands of <i>A. alba</i>	Species-level
<i>Avicennia marina</i>	Dominant, homogeneous and dense stands of <i>A. marina</i> with mixed stands of <i>A. alba</i> , <i>A. officinalis</i> , <i>Aegiceras corniculatum</i> , <i>Ceriops</i> species, <i>Bruguiera</i> species, <i>Excoecaria agallocha</i> , <i>Acanthus ilicifolius</i> and <i>Derris</i> species	Community-level
<i>Avicennia Mixed</i>	Sparsely distributed and stunted <i>Avicennia</i> stands mixed with mangrove associates like <i>Suaedasp.</i> , <i>Sesuvium</i> sp. and <i>Acanthus ilicifolius</i>	Community-level
<i>Aegialitis Mixed</i>	<i>Aegialitis rotundifolia</i> stands mixed with <i>E. agallocha</i> , <i>A. marina</i> , <i>Aegiceras corniculatum</i> and <i>Ceriops</i> species	Community-level
<i>Excoecaria agallocha</i>	Dominant and dense stands of <i>E. agallocha</i> mixed with patches of <i>Ceriops</i> species and <i>Aegiceras corniculatum</i>	Community-level
<i>Phoenix paludosa</i>	Dominant and dense stands of <i>P. paludosa</i> with mixed patches of <i>E. agallocha</i> , <i>Heritiera fomes</i> , <i>Ceriops</i> species, <i>Aegiceras corniculatum</i>	Community-level
Marsh Vegetation	<i>Suaedasp.</i> , <i>Sesuvium</i> sp., <i>Salicornia brachiata</i> , <i>Acanthus ilicifolius</i> and sparsely distributed and stunted <i>A. marina</i> trees	Eco-morphological zonation-level
Saline Blank	Form as a result of increase in salinity due to increase in elevation, probably because of deposition. Composed of sparse and much stunted <i>Avicennia</i> sp. trees	Eco-morphological zonation-level
Intertidal mudflat	Tidal flats that form in the intertidal areas where sediments get deposited by tides or rivers.	Eco-morphological zonation-level

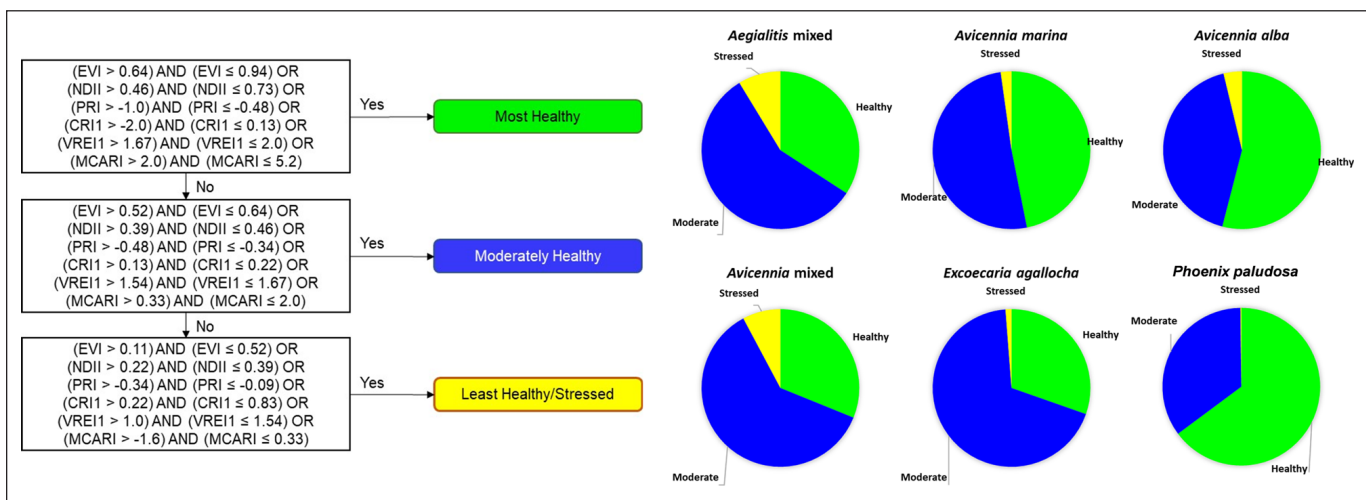


Figure 14.4: Rules for identifying health of the mangroves using DT and proportion of healthiness for the different mangrove classes

15. Generation of geospatial database for notified forest lands of Karnataka State

Karnataka is the first state to adopt geospatial approach for generation of reliable spatial database indicating the boundaries of notified forest lands and to provide institutional mechanism for dissemination of information to various stakeholders. A Standard Operating Procedure (SOP) was developed during the pilot phase of study. With successful conclusion of the pilot study, a state level project is initiated to generate uniform GIS database for all notified forest lands using high resolution remote sensing satellite data (HRS), village cadastral maps, GAGAN based GCPs from field survey to publish georeferenced forest maps for easy reference for general public.

The major activities of the project include creation of ortho-products of HRS data and rapid collection of GCPs in the field

using the GAGAN based GPS device, georeferencing & edge matching of cadastral maps, and generation of seamless mosaic of these maps at different administrative hierarchy. High resolution Cartosat-1 (2.5m) and Resourcesat LISS-IV (5.0m) datasets corresponding to February-April months were orthorectified using GCPs from GCP library. The notified forest lands boundary corresponding to each village is transferred to cadastral maps and verified by respective range forest officer for generation of notified forestland map for each village. Georeferencing of cadastral maps, notified forest maps and cadastral maps in vector format is carried out using GAGAN based GCPs and few tie points from the ortho-image.

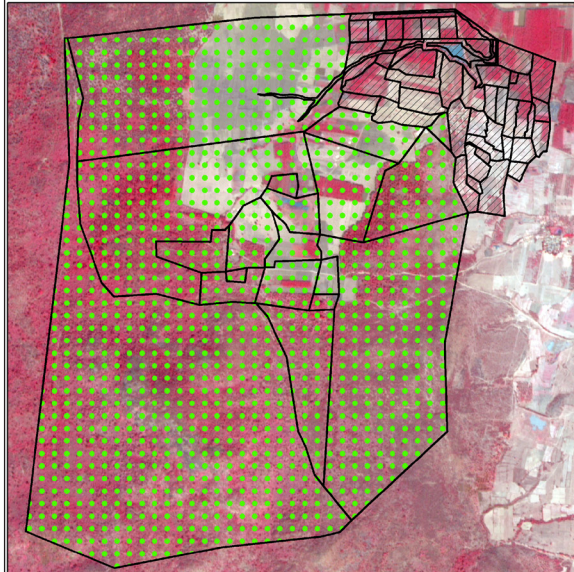
The geo-referenced maps were overlaid on the orthorectified data to check the extent of matching between cadastral maps and ortho images. In case of any mis-match, additional GCP survey was carried out. After quality checking of cadastral maps, edge matching of adjacent village maps was carried out by Karnataka Forest Department using GCPs collected along with



village boundary and *hissa maps*. Field verification of each village maps was carried out by respective forest range officers. The georeferenced cadastral and forest lands maps were mosaicked at forest range and division-wise to generate seamless GIS database. The georeferenced cadastral maps are overlaid on the high-

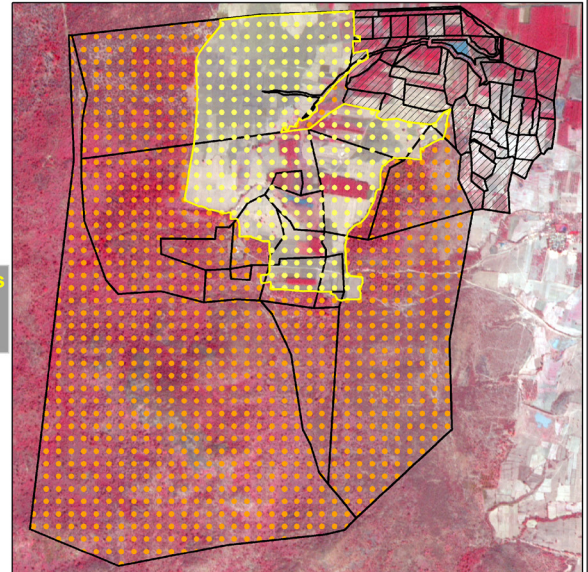
resolution data for reconciliation of forest land boundaries based on the present ground situations captured from the high-resolution satellite data (Figure 15.1). Generation of geospatial database for about 6500 villages have been completed so far and work is in progress for additional 3500 village cadastral maps.

Basavapura Village, Bhadravati Forest Division, Karnataka



Forest Lands as per Notification = 1552.1 ha

Converted Forest Lands
Existing Forest Lands
Notified Forest Lands



Existing notified forest lands = 793.2 ha

Figure 15.1: Reconciliation of notified forest land boundary at cadastral level - Basavanapura village

16. Site suitability for groundwater recharge in hard-rock basaltic terrain

Total 90% of rural Indian resident population is dependent on groundwater for drinking and domestic purposes. In the last four decade or so, the country has witnessed a drastic increase in groundwater demand due to agricultural revolution, rapid population growth and industrial development. This unrealistic and huge demands lead to unplanned abstraction without proper emphasis in recharging capacities of an aquifer and other geo-environmental factors. Artificial groundwater recharge (AGWR) is considered as a strategy to improve the groundwater resources and sustainability as well as existence of a groundwater regime. Hence, in present scenario, any groundwater management techniques must include AGWR depending upon contributing factors such as lithology, geomorphology, lineament, slope, elevation, soil and associated land-use. Conceptually AGWR is a coupled effect of surface and subsurface variables, but in basaltic province sub-surface geology plays the major role to control the recharge phenomena. Integrated use of subsurface stratigraphic model based on well log and field data is of utmost importance for 3-dimensional visualization and assessment of critical basaltic aquifers to maintain the balance between groundwater abstraction and recharge.

The Bhalki watershed of Bidar district, Karnataka has been facing severe water shortage for both irrigation and drinking water purposes for the last few years, which has been further worsened by limited rainfall. In the pre-monsoon season the water problem is aggravated causing severe water scarcity. This, in turn, affects the socio-economic well-being of the resident population.

In the present study, various contributing factors responsible for groundwater recharge like lithology, geomorphology, drainage density, lineament density, slope, soil, land use and sub-surface aquifer characteristics were integrated depending on their decisive contribution to groundwater recharge by geospatial techniques. The adopted knowledge guided approach has added an opportunity to integrate groundwater-related data for better understanding of groundwater and surface water interaction for groundwater replenishment. The study showcased three categories of recharge zones 'highly-suitable', 'moderately suitable' and 'unsuitable'. The recharge zones are found to be in agreement with the observed pre / post-monsoon groundwater table and have good correlation with Electrical Resistivity Tomography (ERT) results (Figure 16.1). This work will be helpful to delineate groundwater recharge zones in similar geological provinces for ensuring water security. Despite all the natural limitations, this study is a valuable practice tool for solving real world water problem.

RESPOND Programme

NRSC RESPOND Basket - 2021 comprising most important research areas for academia is available at https://nrsc.gov.in/Respond_Basket. Last date for submitting the proposals by academia is 15th March, 2021.

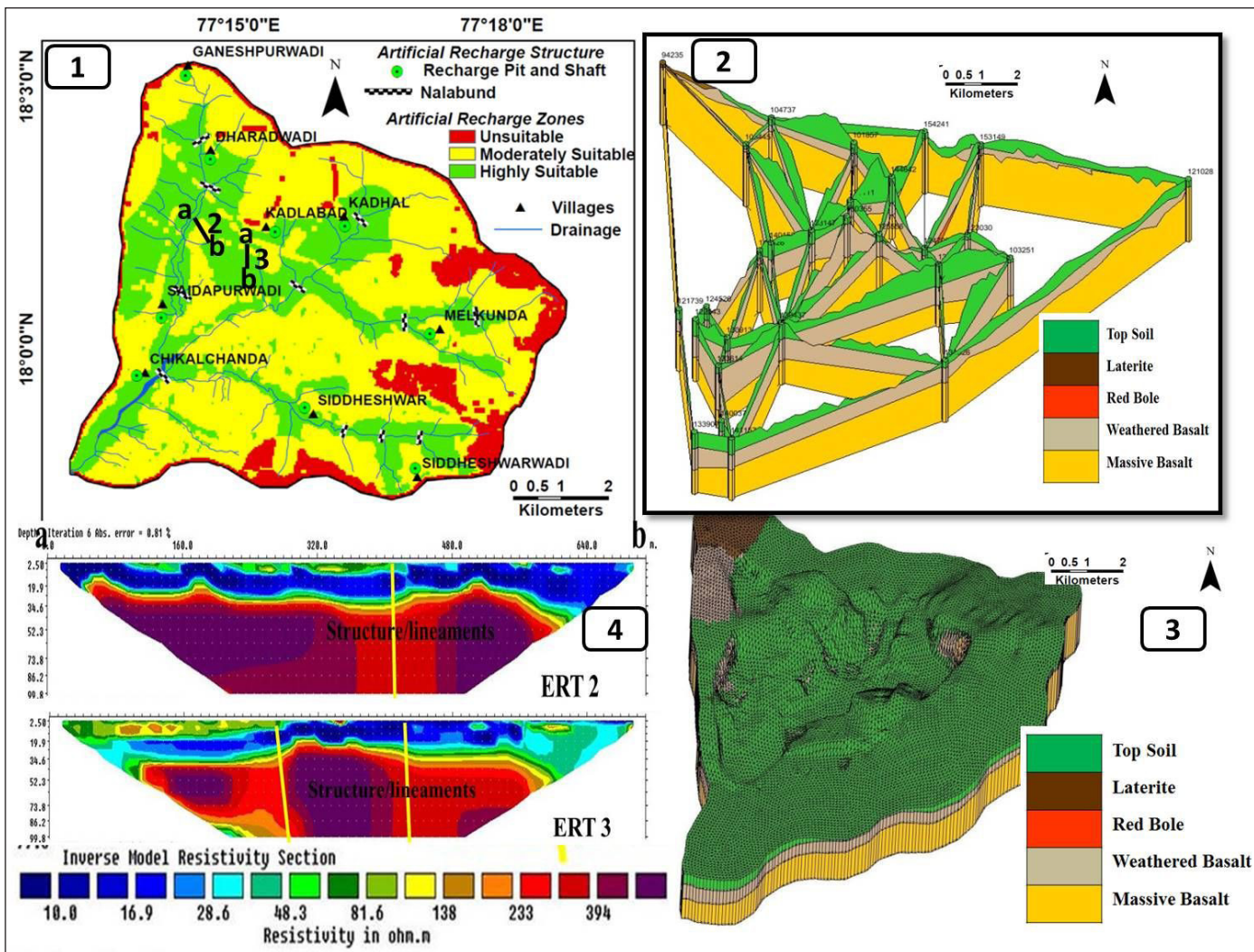


Figure 16.1: Site suitability map for groundwater recharge with probable Artificial recharge Structures; (2) Aquifer cross-sectional and ence diagram for the study area; (3) 3D subsurface stratigraphic model of the study area; (4) ERT cross-section along profile 2 and 3.

TRAINING PLANNER January to June 2021

2021	M	T	W	T	F	S	S	M	T	W	T	F	S	S	M	T	W	T	F	S	S	M	T	W	T	F	S	S	M	T						
January					1	2	3	4	5	6	7	8	9	10	11	12	13	14	15	16	17	18	19	20	21	22	23	24	25	26	27	28	29	30	31	
February	1	2	3	4	5	6	7	8	9	10	11	12	13	14	15	16	17	18	19	20	21	22	23	24	25	26	27	28								
March	1	2	3	4	5	6	7	8	9	10	11	12	13	14	15	16	17	18	19	20	21	22	23	24	25	26	27	28	29	30	31					
April				1	2	3	4	5	6	7	8	9	10	11	12	13	14	15	16	17	18	19	20	21	22	23	24	25	26	27	28	29	30			
May						1	2	3	4	5	6	7	8	9	10	11	12	13	14	15	16	17	18	19	20	21	22	23	24	25	26	27	28	29	30	31
Jun		1	2	3	4	5	6	7	8	9	10	11	12	13	14	15	16	17	18	19	20	21	22	23	24	25	26	27	28	29	30					

NHP : National Hydrology Project
DM : Disaster Management
BO : Bhuvan Overview
HS RS : Hyper Spectral Remote Sensing
GST : Geospatial Technologies



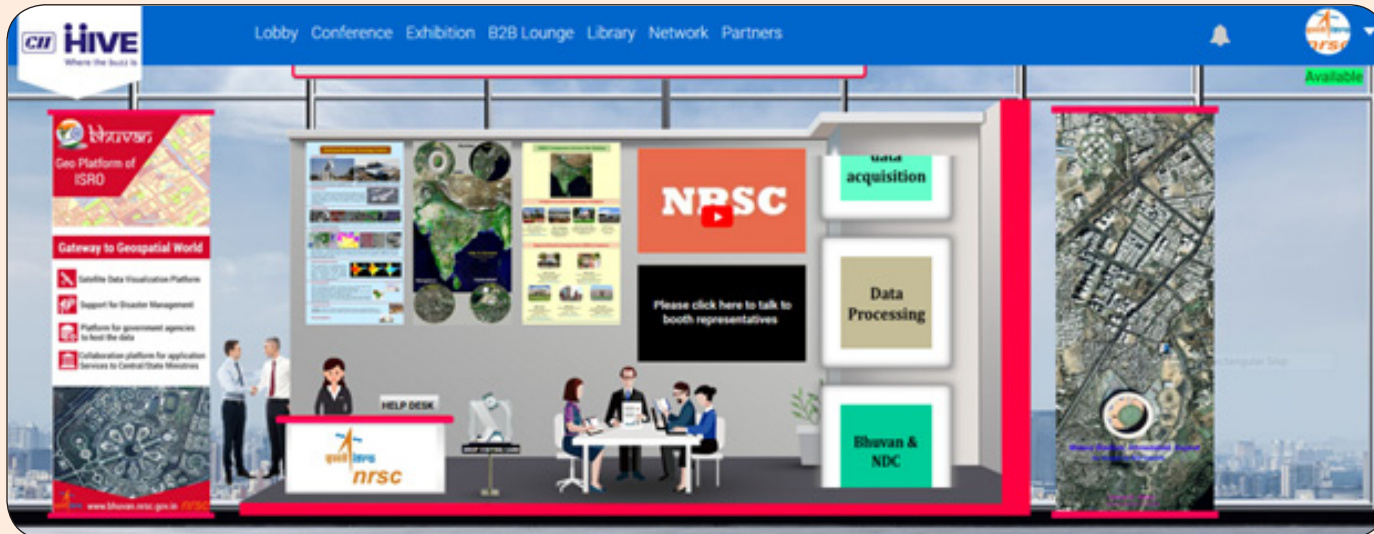
Training and Outreach (Virtual Mode)

162 officers were trained under 5 web based trainings

2069 students were reached under outreach activity

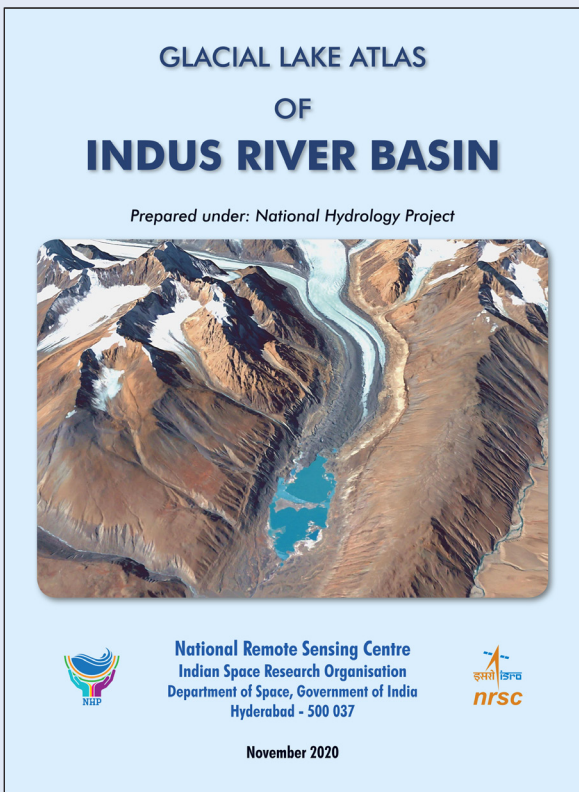
World Space Week: NRSC celebrated World Space Week 2020 in virtual mode and organized audio lectures from Dr R R Navalgund (Satellites improve life – Theme of WSW – 2020), Dr Ashish Goel (The exciting ocean worlds of the solar system), Dr Shaneeth, VSSC (Beyond the blue sky), Ms Aswathy R Krishnan, IISU (Who steers the rocket), Mr Chellathurai, IPRC (Liquid propellants for satellites and launch vehicles), Mr B V Subbarao, SDSC (Space debris), Ms G Umadevi, NRSC (Satellite data reception) and Mr Vinod M Bothale, NRSC (Remote Sensing Satellite data products generation).

International Space Conference & Exhibition (2020) - NRSC stall in the virtual conference



Release of “Glacial lake atlas of Indus river basin” prepared under National Hydrology Project

The atlas was formally released by Shri. U.P. Singh Secretary, Ministry of Jal Shakti and Shri Santanu Chowdhury, Director, NRSC on 2nd Dec, 2020 through video conference workshop.



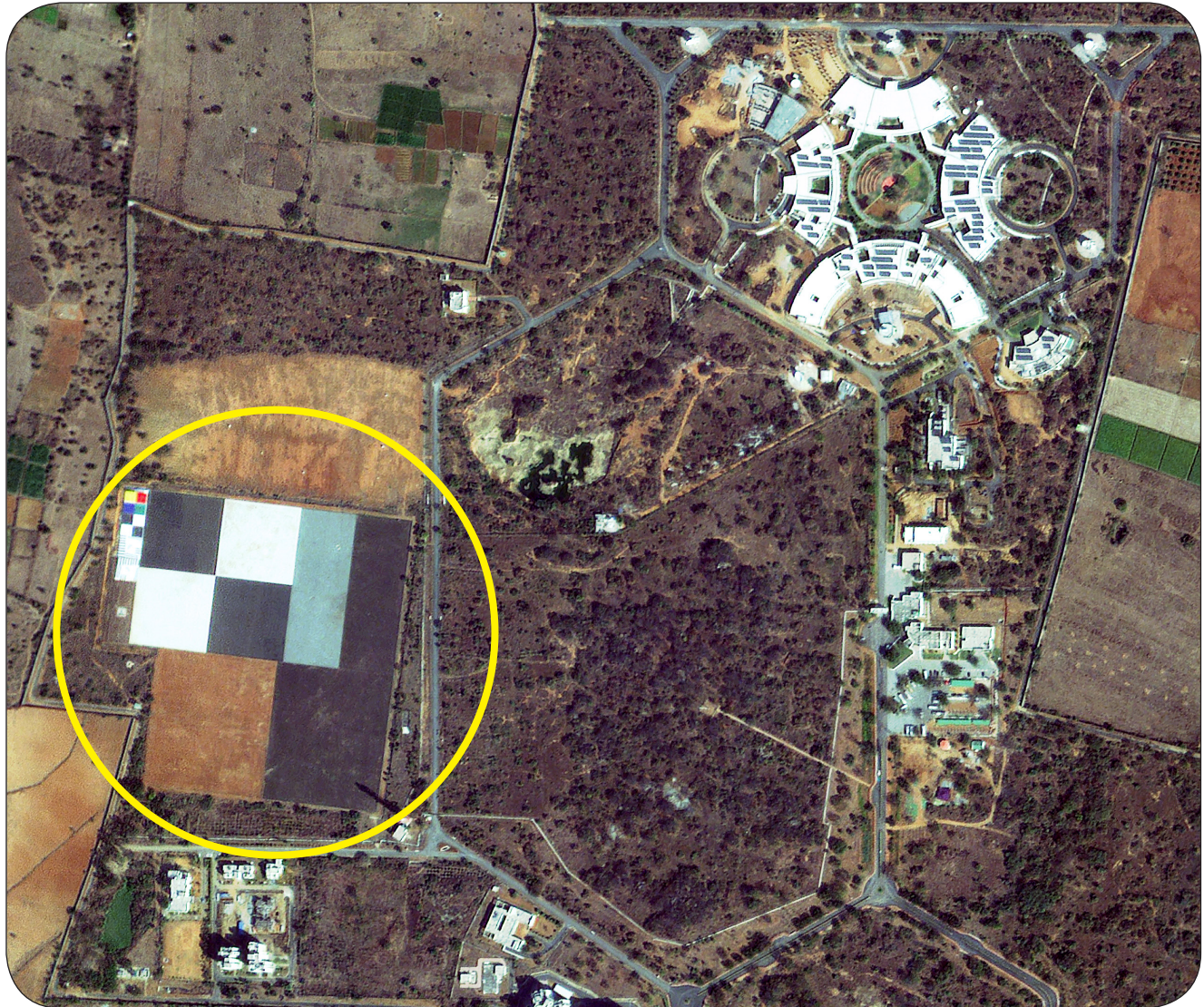
Publications:

- Anand, A., Krishnan, P., Suryavanshi, A. S., Choudhury, S. B., Kantharajan, G., Srinivasa Rao, Ch., Manjulatha, C. and Babu, D. E. (2020). Identification of suitable aquaculture sites using large-scale land use and land cover maps factoring the prevailing regulatory frameworks: A case study from India. *Journal of the Indian Society of Remote Sensing*, <https://doi.org/10.1007/s12524-020-01211-7>
- Bhadra, B.K., Pathak, S., Nanda, D., Gupta, A., Srinivasa Rao, S. (2020). Spectral Characteristics of Talc Mineral and its Abundance Mapping in Jahazpur Belt of Rajasthan, India using AVIRIS-NG Data. *International Journal of Remote Sensing*. 41, (22), pp.8754-8774
- Chattoraj, S. L., Prasad, G., Sharma, R. U., Champati Ray, P. K., van der Meer, F. D., Guha, A., & Pour, A. B. (2020). Integration of remote sensing, gravity and geochemical data for exploration of Cu-mineralization in Alwar basin, Rajasthan, India. *International Journal of Applied Earth Observation and Geoinformation*, 91, 102162. <https://doi.org/10.1016/j.jag.2020.102162>
- Chaudhury, S., GuhaArindam, Bhaumik A. Rani. K. (2020) Potential Utility of Reflectance Spectroscopy in Understanding the Paleocology and Depositional History of Different Fossils”, *Scientific Report, Nature* <https://doi.org/10.1038/s41598-020-73719-4>
- Devi, A.R., Reddy, C.S. & Shimrah, T. (2020). Assessment of forest fragmentation in a traditional shifting agricultural landscape in Senapati District of Manipur, Northeast India. *Environment, Development and Sustainability*. <https://doi.org/10.1007/s10668-020-01059-4>.
- Durga Rao, K H V, Shrivavya, A, and Dadhwal, V K. (Aug 2020). Satellite Based River Discharge Estimation using River Hydraulic Geometry through Genetic Algorithm Technique. *Journal of Hydrology*. 589 (2020), <https://doi.org/10.1016/j.jhydrol.2020.125361>
- Giribabu, D., Manish, V., Srinivasa Rao, S., Jha, C.S. (2020). Geospatial Opinion on Unusual Locust Swarm Invasions during Amphan Cyclone. *Journal of Geoscience and Environment Protection*, 8, 144-161
- Giribabu, D., Verma, M., Srinivasa Rao, S. (2020). Evaluation of best-fit terrain elevation of ICESat-2 ATL08 using DGPS surveyed points. *Journal of Applied Geodesy*, 14, (3), 285-293
- Giribabu, D., Verma, M., Satyanarayana, P., Srinivasa Rao, S. (2020). Evaluation of ICESat-2 ATL08 Data Product: Performance Assessment in Inland Water. *European Journal of Environment and Earth Sciences*, 1(3)
- Giribabu, D., Bera, A.K., Srinivasa Rao, S., Jha, C.S. (2020). Earth Observation Satellites for Locust Surveillance, *Geography and You*
- Giribabu, D., Srinivasa Rao, S. (2020). Validation of ICESat-2 surface water level product ATL13 with near real time gauge data. *Hydrology*, 8(2). 19-25
- Guha, Arindam, Chattoraj, S. Chatterjee, S., Bhaumik, S. Vinod Kumar, K. (2020) Reflectance spectroscopy guided broadband spectral derivative approach for delineating glauconite rich zones within fossiliferous limestone, Kachchh region, Gujarat, India, *Ore Geology Reviews*, Vol.128, 103818 <https://doi.org/10.1016/j.oregeorev.2020.103818>
- Guha, Arindam, Saw, A. K., Mukherjee, A., Verma, C. B., Kumar, K. V., & Diwakar, P. G. (2020). Eigenvector analysis derived Landsat OLI principal components and reflectance spectra guided constrained energy minimization maps for Iron exploration in Siddhi, Madhya Pradesh. *Geocarto International*, 1-13. <https://doi.org/10.1080/10106049.2020.1801861>
- Guha, Arindam, Chatterjee S., Ooman, Thomas, Vinod Kumar, K. (2020). Synergistic use of ASTER, L-band ALOS PALSAR and Hyperspectral AVIRIS-NG Data for Geospatial Exploration of lode type gold deposit – a study in Hutti-Schist Belt, India. *Ore Geology Reviews*, Vol. 127, 103825 <https://doi.org/10.1016/j.oregeorev.2020.103825>
- Gupta, S., Dharmaraj, T., Reddy, K. M., & Ravisankar, T. (2020). Spatial-Temporal Analysis and Visualization of Rural Development Works Implemented Under World's Largest Social Safety Programme in India - a Case Study. *Journal of Geovisualization and Spatial Analysis*, 4(2), 1-14. <https://doi.org/10.1007/s41651-020-00062-7>
- Hareef Baba Shaeb, K., Biswadip, G., Dutta, D., Choudhury, S. B., & Seshasai, M. V. R. (2020). Spatial variability of the aerosol optical thickness over Southern Ocean and coastal Antarctica: Comparison with MODIS and MERRA-2 aerosol products. *Deep Sea Research Part-II: Topical Studies in Oceanography*, 104776. <https://doi.org/10.1016/j.dsr2.2020.104776>
- Jain, J., & Mitran, T. (2020). A geospatial approach to assess climate change impact on soil organic carbon in a semi-arid region. *Tropical Ecology*, 61(3), 412-428. <https://doi.org/10.1007/s42965-020-00100-x>
- Krishnapriya M, Nayak R K, Shaik Allaudheen, A. Bhuvana Chandra, M V R Shesasai, C S Jha, V. K. Dadhwal, S K Sasma, K V R. Prashad (2020), Seasonal variability of tropospheric CO₂ over India based on model simulation, satellite retrieval and in-situ observation, *Journal of Earth System Sciences*, Vol.129 211 doi:10.1007/s12040-020-01478-x
- Lima, C. B., Prijith, S. S., Rao, P. V. N., Sai, M. V. R. S., & Ramana, M. V. (2020). Quality Estimates of INSAT-3D Derived Cloud Top Temperature for Climate Data Record. *IEEE Transactions on Geoscience and Remote Sensing*, 1-6. <https://doi.org/10.1109/tgrs.2020.3022680>
- Mandal, A., Majumder, A., Dhaliwal, S. S., Toor, A. S., Mani, P. K., Naresh, R. K., Gupta, R. K., & Mitran, T. (2020). Impact of agricultural management practices on soil carbon sequestration and its monitoring through simulation models and remote sensing techniques: A review. *Critical Reviews in Environmental Science and Technology*, 1-49. <https://doi.org/10.1080/10643389.2020.1811590>
- Nagajothi K, Rajashekara, H.M and B. S. Daya Sagar B.S (2020). IGARSS 2020 Quantitative Analysis Of Watersheds Partitioned From Cartosat Dem Of Lower Indus Sub-Basin via Multi-fractal Spectra
- Prijith, S.S., K. Srinivasarao, C.B. Lima, B. Gharai, P.V.N. Rao, M.V.R. Seshasai, M.V. Ramana (2020) Effects of land use/land cover alterations on regional meteorology over Northwest India, *Science of Total Environment*, <https://doi.org/10.1016/j.scitotenv.2020.142678>
- Priyadarshi N., Bandyopadhyay, S., Chowdhary, V.M., Chandrasekar, K., Jeganathan, C., Srivastava, Y.K., Raj, U. & Jha, C.S. (2020). Segmentation-based approach for trend analysis and structural breaks in rainfall time series (1851-2006) over India, *Hydrological Sciences Journal*, 65:9, and 1583-1595. <https://doi.org/10.1080/02626667.2020.1761022>
- Ramesh Pudi, Priyom Roy, Tapas R. Marthar and K. Vinod Kumar (2020) Estimation of earthquake local site effects using microtremor observations for the Garhwal-Kumaun Himalaya, India. *Near Surface. Geophysics* 08 October 2020 <https://doi.org/10.1002/nsg.12128>
- Reddy, C.S., Kurian, A, Srivastava, G., Singhal, J., Varghese, A.O., Padalia, H., Ayyappan, N., Rajashekar G., Jha, C.S. & Rao, P.V.N. (2020). Remote Sensing Enabled Essential Biodiversity Variables for Biodiversity assessment and monitoring: Technological development and potentials. *Biodiversity and Conservation*. DOI 10.1007/s10531-020-02073-8
- Reddy, C.S., Gija, A.A., Anuja J. & Sabu, M.M. (2020). Micro Hotspots of New Species Discoveries in India: Flora and Fauna. *Current Science*. 191(1), 1408-1410
- Roy P, Singh S, Vinod Kumar K. (2020). Topographic control on the recession of the Kokthang glacier and its effect on proglacial lake dynamics. *SN Applied Sciences* volume 2, Article number: 1988 (2020) <https://doi.org/10.1007/s42452-020-03727-6>
- Sai Charan, Vasala, Naga Jyothi B, Rajarshi, Tushar Wankhede, I.C Das, Jand. Venkatesh4, (2020) An Integrated Geohydrology and Geomorphology Based Subsurface Solid Modelling for Site Suitability of Artificial Groundwater Recharge: Bhalki Micro-watershed, Karnataka, *Journal Geological Society in India*, (Nov, 2020)
- Satyesh Ghetiya, Nayak R.K. (2020), Genesis Potential Parameter using satellite derived daily Tropical Cyclone Heat Potential for North Indian ocean, *International Journal of Remote Sensing*, 41(23), p8934-8947, <https://doi.org/10.1080/01431161.2020.1795299>
- Subbarao, N.V.V.S.S.T., Mani, J.K., Shrivastava, A., K. Srinivas and A. O. Varghese. (2020). Acreage estimation of kharif rice crop using Sentinel-1 temporal SAR data, *Spatial Information Research*, <https://doi.org/10.1007/s41324-020-00374-2>
- Unnikrishnan, A. & Reddy, C.S. (2020). Characterizing distribution of Forest Fires in Myanmar using Earth Observations and Spatial Statistics Tool. *Journal of the Indian Society of Remote Sensing*, 48(2), 227-234. <https://doi.org/10.1007/s12524-019-01072-9>
- Kanchana A.L, Vijay Kumar Sagar, Mahesh Pathakoti, D.V. Mahalakshmi, K. Mallikarjun & Biswadip G (2020); Ozone variability: Influence by its precursors and meteorological parameters- an investigation *Journal of Atmospheric and Solar-Terrestrial Physics*, <https://www.sciencedirect.com/science/article/pii/S1364682620302716>

About Calval site, IMGEOS, Shadnagar

The in-house integrated and instrumented IMGEOS Cal-Val facility, spread across 300m x 200m is operationalised in 2015 at IMGEOS Shadnagar campus. The 5 types of natural targets, stone and soil materials artificially laid in the facility provide opportunity of (i) Vicarious calibration of Space borne/Air borne multi spectral sensors for mid and high resolution and optical sensors upto 30m resolution & (ii) Spatial characterisation of high and very high resolution optical data upto 6m in terms of Modulation Transfer function (MTF). This facility also provides opportunity of Microwave data calibration with well characterised Square tri hedral and di hedral Corner Reflectors for SAR data. By virtue of natural thermal gradients of different materials, these targets can also be used for thermal data radiometric response study.

Customised targets, like mirrors and cloth based, are also being designed and developed for very high resolution Carto data spatial characterisation in terms of SWR (Square Wave Response) and PSF (Point Spread Function). The well geometrically calibrated very high resolution GCP facilitates the resolvable pixel size on the ground. These well geometrically characterised targets are also useful in establishing the geometric accuracy of high and very high resolution data.



Calval site as viewed by Cartosat-2E, Date of pass: 7th February 2020

P2P Editorial Board

Dr. Rajashree Bothale
P. Krishnaiah
Dr. Tapas Ranjan Martha
R. V. G. Anjaneyulu

Dr. M.V. Ramana
M. Arulraj
J. Narendran
Seema Kulkarni

A. Chalapati Rao
Dr. A. K. Bera
Dr. A. O. Varghese

Dr. V. M. Chowdhary
Ramachandra Hebbar
E. Vijayasekhar Reddy

National Remote Sensing Centre
Indian Space Research Organisation
Dept. of Space, Govt of India
Balanagar, Hyderabad - 500 037
www.nrsc.gov.in

Feedback

Please post your comments to:
p2p@nrsc.gov.in

ISSN 0974 9802